Direction de l'énergie nucléaire
Centre de Cadarache
Département d'études des combustibles
Service d'études et de simulation du comportement des combustibles

CEA/DEN/CAD/DEC/SESC
DO 123 05/07/10
10PPJP000179

CADARACHE Note Technique

PRELIMINARY QUALIFICATION OF THE ATLAS V3.0 CODE - EXPERIMENTS HFR-EU1BIS AND NPR-1
QUALIFICATION PRÉLIMINAIRE DU CODE ATLAS V3.0 - EXPÉRIENCES HFR-EU1BIS ET NPR-1

CEA/DEN/CAD/DEC/SESC/LSC NT10-021 – Indice 0

April 2010

SOLÈNE GICQUEL PETIT*, LAURENT GAUTHIER*

* CDD RAPHAEL

Commissariat à l'Énergie Atomique
Centre : Cadarache
Adresse : DEC/SESC/LSC- Bât. 151 - 13108 Saint Paul Lez Durance
Tél. : 04 42 25 38 62 Fax : 04 42 25 29 49 Couriel : sesclsc@drncad.cea.fr
Établissement public à caractère industriel et commercial - RCS Paris B 775 685 019

NIVEAU DE CONFIDENTIALITÉ

DO	DR	CCEA	CD
X			

CLIENTS

PARTENAIRES/CLIENTS	ACCORD	TYPE D'ACTION
European Commission	6ième PCRD (FP6)	RAPHAEL integrated project

RÉFÉRENCES INTERNES CEA

DIRECTION D'OBJECTIFS	DOMAINE	PROJET	EOTP
DISN	R4G	RAPHAEL	A-ASYST-06-05

JALON	INTITULÉ DU JALON	DÉLAI DE CONFIDENTIALITÉ CONTRACTUELLE	CAHIER DE LABORATOIRE
	Sans objet	Permanent	—

SUIVI DES VERSIONS

INDICE	DATE	NATURE DE L'ÉVOLUTION	PAGES,CHAPITRES
0	27/04/10	Émission initiale	50

	NOM	VISA	DATE
RÉDACTEUR	S. Gicquel Petit	Gicquel Petit	27.04.2010
VÉRIFICATEUR	F. Michel	F. Michel	27.04.2010
APPROBATEUR	R. Masson		29/04/2010
ÉMETTEUR	E. Touron	P.I. M. Casella	15/6/2010

Ce document contient des résultats issus de travaux réalisés dans le cadre de l'accord 6ième PCRD (FP6) CEA - European Commission. Sa diffusion est soumise aux règles de cet accord.

MOTS CLEFS

RAPHAEL, HTR, Fuel particle, Atlas, HFR-EU1bis, NPR-1.

RÉSUMÉ / CONCLUSIONS

La qualification du code ATLAS est le livrable D-FT4.9 du projet européen RAPHAEL. Ce document regroupe les résultats d'une qualification préliminaire du code ATLAS V3.0, en présentant les données, sollicitations et une partie des résultats expérimentaux des expériences HFR-EU1bis et NPR-1, ainsi que les résultats de calcul fournis par le code ATLAS V3.0. Cette qualification a été réalisée en s'appuyant sur le jeu de modèles et de propriétés "RAPHAEL2008".

Summary

The qualification of the ATLAS code is the deliverable D-FT4.9 of the RAPHAEL Project. This document merges the results of a preliminary qualification of the ATLAS V3.0 code, by gathering the data, loads and some experimental results of the HFR-EU1bis and NPR-1 experiments, along with the calculated results provided by the ATLAS V3.0 code. This qualification has been made using the "RAPHAEL2008" set of models and properties.

LISTE DE DIFFUSION

Diffusion externe

SOCIÉTÉ	NOM DU DESTINATAIRE	NOMBRE D'EXEMPLAIRES	OBSERVATIONS
AREVA NP	E. BOGUSCH	@	@ RAPHAEL Project: document disponible sur le site SINTER, avec alerte par mail
	L. DANIEL	1	
	P. GUILLERMIER	1	
	D. HITTNER	1	
	P. MAILHE	@	
	M. PASQUET	1	1 : Diffusion CD-ROM
	L. GAUTHIER	1	
ITU	D. BOTTOMLEY	@	
	A. KELLERBAUER	@	
FZJ	H. NABIELEK	@	
	K. VERFONDERN	@	
IRSN/Cadarache	R. DUBOURG	@	
	M. KISSANE	@	
JRC	M. FUTTERER	@	
	T. OJALA	@	
	H.H. OVER	@	
NNL	T. ABRAMS	@	
	D. EVERY	@	
NRG	S. DE GROOT	@	

Diffusion interne

DPT/SERVICE/LABO	NOM DU DESTINATAIRE	NOMBRE D'EXEMPLAIRES	OBSERVATIONS
DISN/R4G	F. GAUCHE	1	1 : Intranet CEA
	J. ROUAULT	1	
DTN/SMTM/LMN	P. BERNARD	1	
	C. ROURE	1	
DEC	P. BROSSARD	I	I : Note sur serveur INTRADEC (avec alerte mail)
	M. TOURASSE	I	
DEC/CP	P. OBRY	I	
	V. BASINI	I	
DEC/SA3C	F. SUDREAU	I	
	G. DUCROS	I	
DEC/SA3C/LARC	C. GUY	I	
	A. LABET	I	
DEC/SPUA	S. CAMARO	I	
DEC/SPUA/LCU	M. BROTHIER	I	
	G. KYRIADZI	I	
DEC/SESC	E. TOURON	I	
	M. CASELLA	I	
DEC/SESC/LIPA	M. PHELIP	I	
	T. LAMBERT	I	
	D. PARRAT	I	
DEC/SESC/LSC	R. MASSON	I	
	M. PELLETIER	I	
	F. MICHEL	I	
	C. BONHOMME	I	

TABLE OF CONTENTS

ABBREVIATIONS

ATLAS	Advanced Thermal mechanical Analysis Software code developed to support the HTR reactor and fuel R&D program
AVR	Arbeitsgemeinschaft VersuchsReaktor - Jülich
BAF	Bacon Anisotropy Factor
BU	Burn Up, total energy released by mass unit in a fuel (MWday $/\mathrm{t}^{-1}$)
CEA	Commisariat à l'Énergie Atomique
EFPD	Equivalent Full Power Days
EOL	End Of Life
FIMA	Ratio of metallic atoms which have already undergo the fission reaction per the number of initial metallic atoms
%FIMA	%FIMA = FIMA * 100
GLE	Fuel elements with low-enriched UO_2 particles (AVR)
HEU	High-Enrichment Uranium (about 3%)
HFIR	High Flux Isotope Reactor
HFR	High-Flux Reactor (Petten, Holland)
INEEL	Idaho National Engineering and Environmental Laboratory
HTR	High-Temperature Reactor
IPyC	Inner Pyrocarbon
JRC	Joint Research Centre
LEU	Low-Enrichment Uranium
N\A	Not Available or Not Applicable
NP-MHTGR	New Production Modular High Temperature Gas Reactor
NPR	New Production Reactor
OPyC	Outer Pyrocarbon
ORNL	Oak Ridge National Laboratory
PIE	Post-Irradiation Examination
R/B	Release-to-Birth rate
RAPHAEL	ReAcor for Process heat, Hydrogen And ELectricity generation
SiC	Silicon Carbide
TRISO	Tri-coated Isotropic
UCO	Uranium OxyCarbide
VHTR	Very High-Temperature Reactor (over 1000$^\circ\mathrm{C}$for the VHTR concept)

1 INTRODUCTION

1.1 GENERALITIES

This document is a part of the Deliverable D-FT4.9 of the RAPHAEL Project, which aim is to qualify the HTR Fuel Modeling developed in the projects HTR-F and RAPHAEL and integrated in ATLAS. This Modeling corresponds to a particular set of law called "RAPHAEL2008" selected [11] from the models gathered by the project. Data of the European HTR-fuel database, located at the JRC, Petten (`https://odin.jrc.ec.europa.eu/HTR-Fuel-DB/output/login.php`) are directly used thanks to an interface dedicated to ATLAS. The goal of this very document is to present the data, loads and a part of the experimental results of the HFR-EU1bis and NPR-1, along with the calculation results obtained with the code ATLAS V3.0. The statistical method, the law of the failure probability and the Release-to-Birth rate are

more precisely studied.
RAPHAEL is the European integrated project which focuses on the viability and performance issues for the HTR. ATLAS is the CEA software (integrated in the PLEIADES platform) dedicated to the simulation of the fuel of the HTR; it has been chosen as a reference code for this project.

1.2 STRUCTURE

This document is composed of two parts, each one dedicated for one experiment among NPR-1 and HFR-EU1bis. For each of the experiments, the following data are presented:

- a brief description of the experiment (location in the core, shape of the capsule, name of the fuel elements) and all the data that have been gathered of the HTR fuel elements;
- how was constructed the load history, depending on the available data;
- the experimental results used in a further comparison with code results;
- the model assumptions, and eventually differences with the RAPHAEL2008 set of models and properties;
- the calculated results, provided by the ATLAS V3.0 code;
- the comparison between experimental and ATLAS results.

Reasons of the choice of the experiments.

The NPR-1 experiment is used as the first one entered in the database. Its interest lies also in the numerous particle layer failures observed and their probability determination by systematic metallographic examination of hundreds of particles.
The second experiment, HFR-EU1bis, is part of the RAPHAEL project. It is one of the most recent HTR irradiation experiment with recent information, representative of the fuel pebbles produced nowadays. It aims at exploring the potential for high burn-up and high performance of the existing fuel pebbles for application to the conceptual Generation IV VHTR. ATLAS has to be validated on such experiment for a future utilization.

2 NPR1

The NPR-1 experiment was performed by the ORNL in the HFIR reactor under direction of the INEEL. Its objectives were to demonstrate the irradiation performances of American reference NP-MHTGR fuel at the upper bounds of burn-up, temperature and fast fluence. This irradiation was integrated in the NP-MHTGR project.
Almost all the data available for this irradiation were extracted from synthesis documents from MAKI *et al.* [13] and PETTI *et al.* [15].

2.1 DESCRIPTION OF THE EXPERIMENT

2.1.1 Sample Holder

A schematic view of the sample holder is presented on the Figure 1. The sample holder, made of Inconel-718, composed the second containment. The first containment is composed of a single capsule, made of

Inconel-718, containing the 16 compacts which were hold in place by H-451 graphite sample holder.

The capsule is divided into two columns, **column A** and **column B**, as showed on yellow labels on Figure 1, and into zones, numbered from **1** to **4**. Because of these symmetry, it's expected that only four different loads history may be representative of the experiment. It's the assumption made by MAKI *et al.* [13], and it explains that only four histories are presented.
The identification number of the compacts has been changed in the frame of this document (using the names used in other documents on this experiment[1]) and have been called from A1 to B8, as showed on Figure 1.

2.1.2 Loads Control

The fuel particle loadings in each region were varied to compensate for the axial flux distribution in HFIR and allow a more uniform heat generation rate along the capsule. The relative concentration of an helium-neon mixture were adjusted in order to control the compact temperature.

[1]Hopping that names correspond but it can not be checked.

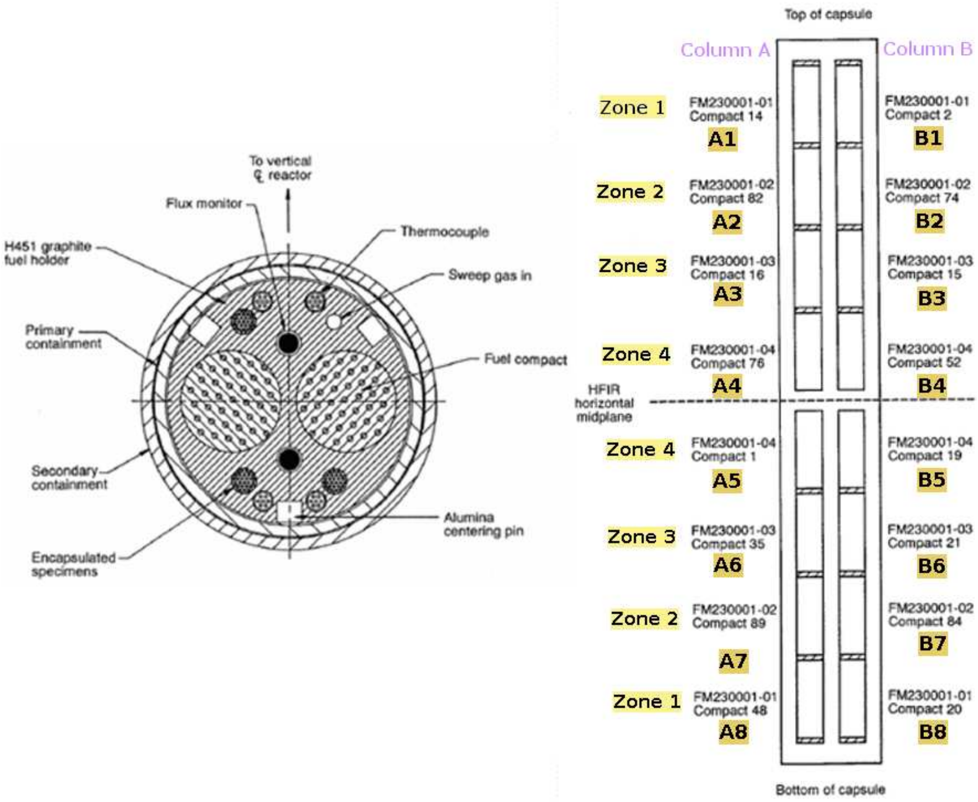

Figure 1: NPR-1 EXPERIMENT SAMPLE HOLDER FROM [13].

2.1.3 Fuel

The HTR fuel inserted in the NPR-1 capsule is from American research for the MP-MHTGR project. It's in shape of compacts in which are inserted **HEU-TRISO** particles with **UCO** kernels, from the '**FM19-00001 composite**' batch. It's assumed that the Graphite matrix was made of Natural Graphite. The characteristics of the batch are summarized on Table 1. The 'mean' and 'standard deviation' were obtained from fabrication measures, the 'Min' and 'Max' values are from the specifications for the fuel of the NPR reactor; all of them summarized by MAKI *et al.* [13] and PETTI *et al.* [15].

Layer	Characteristic	Mean	Standard Deviation	Min	Max
Material	UCO				
Kernel	Enrichment (^{235}U WT%)	93.147	0.007	93.30	94.15
	Radius (μm)	100	2.5	72.5	102.5
	Density ($g.\ cm^{-3}$)	10.51	0.01	10.3	*10.93***
	O/U Atomic ratio (/)	1.5098	0.0066	1.4	1.7
	C/U Atomic ratio (/)	0.3618	0.0008	*0**	0.5
Buffer	Thickness (μm)	101.7	10.2	90	110
	Density ($g.\ cm^{-3}$)	0.9558	0.005	0.80	1.10
IPyC	Thickness (μm)	52.9	3.7	40	60
	Density ($g.\ cm^{-3}$)	1.923	0.008	1.85	1.95
	BAF (/)	1.058	0.005	*1**	1.2
SiC	Thickness (μm)	35.3	3.1	30	40
	Density ($g.\ cm^{-3}$)	3.2278	0.0007	3.18	*3.22**
OPyC	Thickness (μm)	39.1	4.0	30	50
	Density ($g.\ cm^{-3}$)	1.85	0.01	1.80	1.95
	BAF (/)	1.052	0.0062	*1**	*1.2****
Material	Natural Graphite****				
Geometry	Compact				
Fuel Elemeny	Radius (mm)	12.43	N/A	12.37	12.51
	Length (mm)	49.42	0.11	48.8	49.8
	Density ($g.\ cm^{-3}$)	1.8	N/A	N/A	N/A
	Number of particles	4844	0.11	3600	6000
	Last fabrication Temperature ($^\circ$C)	1650	N/A	N/A	N/A

Table 1: CHARACTERISTICS OF THE 'FM19-00001 COMPOSITE' PARTICLE BATCH AND NPR COMPACTS.

* No specification is given, so a value close to the theoretical density has been chosen.
** No specification is given, the theoretical boundary has been chosen.
*** No specification is given. It is assumed to be the same as for IPyC.
**** Assumption.

2.2 HISTORY

2.2.1 Time

The NPR-1 experiment begins on July the 25th, 1991 and was completed on May the 29th, 1992. It lasted 170 full power days during which the fuel was subjected to height cycles. The time history has been extracted from the temperature history as no other data were available on the irradiation history.

2.2.2 Temperature

The axial and azimuthal temperatures at various locations in the capsule were measured by 27 thermocouples, incorporated into 4 thermocouple array tubes inserted in the graphite holder. Fuel temperature was calculated from these measurements.
Calculated temperature history is given by MAKI *et al.* [13] in figure 4.9 of the document, with two data as a function of time: the average and the maximum temperature history for all the compacts in their centre.
The following assumptions were made:

- temperature variations of less than 50$^{\circ}\mathrm{C}$ during a cycle are not taken into account;
- minimum temperature is calculated assuming the same difference between the average and maximum temperatures;
- reactor shutdowns are modelized by temperature decreases during cycles to the temperature reached at the bottom of Figure 4.9 from MAKI *et al.* [13], equals to 700$^{\circ}\mathrm{C}$. Nevertheless, the value of this temperature is not expected to induce much differences;
- as the history is extracted from a figure, uncertainties are expected to be high; this is particularly perceptible for the length of reactors power increases or shutdowns. In order to avoid numerical problems, the obtain temperature versus time history has been slightly modified to have power increases and decreases that last from **12 to 24 hours**.

The temperature range used for these calculations is presented on figure 2.

2.2.3 Fluence

The calculated fluence for each of the zones of the NPR-1 capsule is given by MAKI *et al.* [13] on figure 3. The following assumptions has been taken:

- the average fluence across the different zones of the capsule;
- the maximum and minimum fluence have been calculated as the half of the difference between two zones.

The fluence across the different zones is presented on Figure 3.

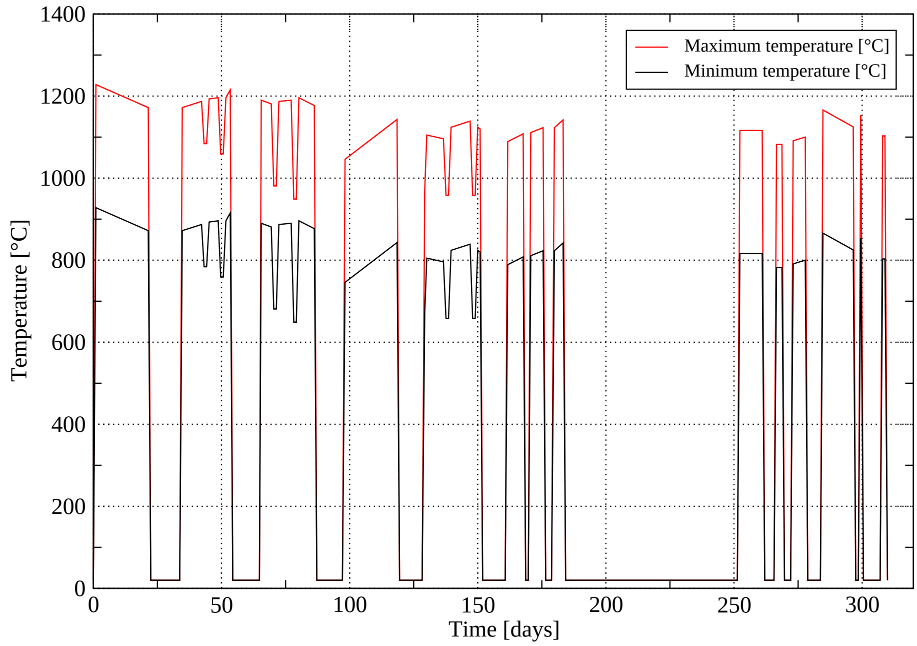

Figure 2: TEMPERATURE RANGE DURING THE NPR-1 EXPERIMENT.

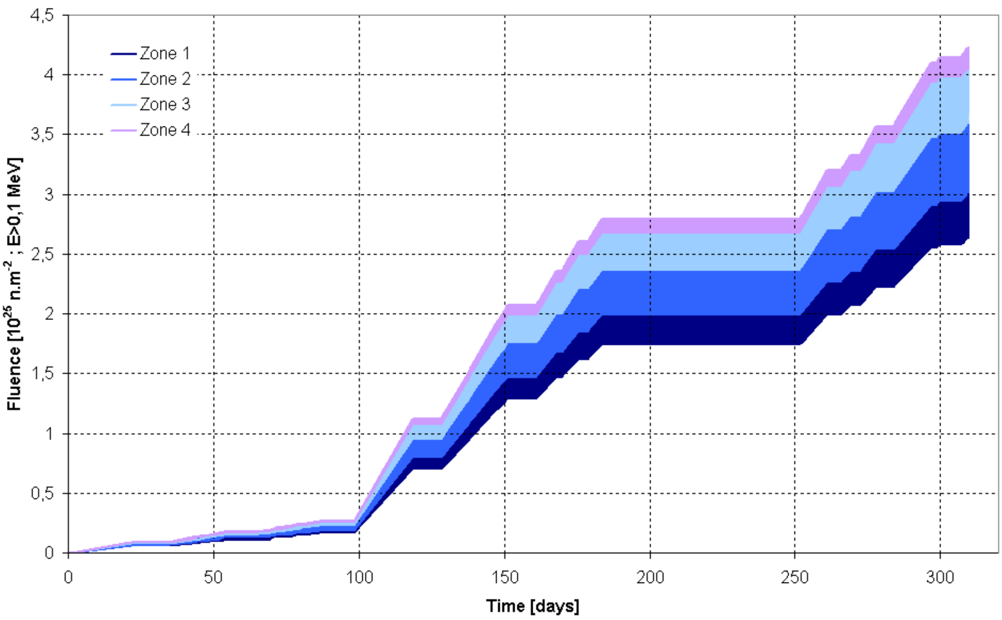

Figure 3: CYCLES AND FLUENCE FOR THE NPR-1 EXPERIMENT.

2.2.4 Burn-up

The calculated burn-up versus fluence for each of the zones of the NPR-1 capsules is given by MAKI *et al.* [13] on Figure 4.11. In order to use these data to construct a history, it's necessary to model the curves on this figures. The data from [13] and the modeled curves, made with piecewise linear functions, are presented on Figure 4; the maximum difference between both curves is about 5%. The modeled curves allowed to construct the calculated burn-up presented on Figure 5.

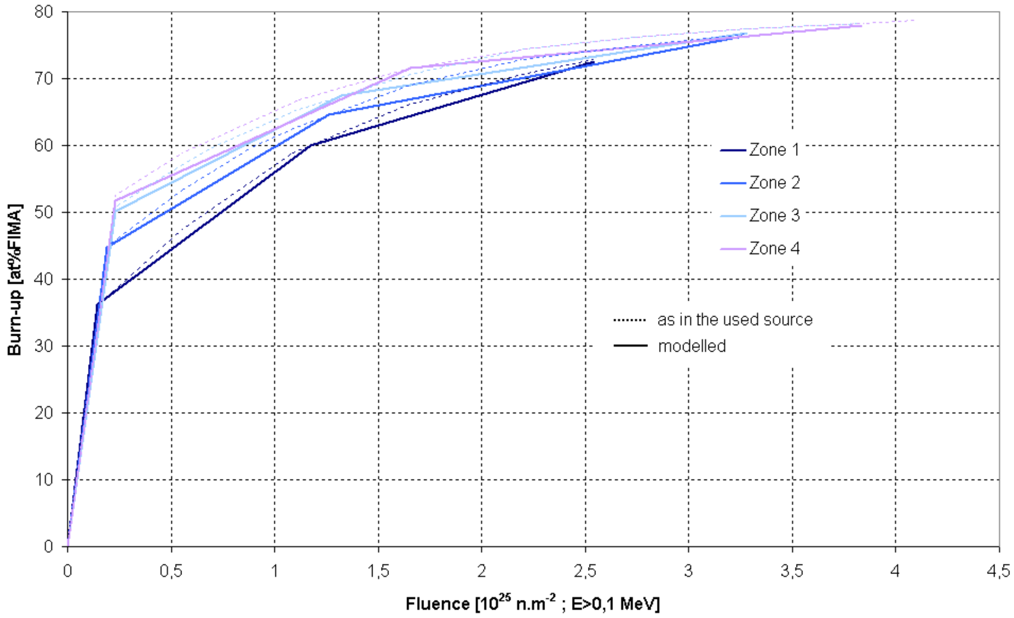

Figure 4: BURN-UP AS A FUNCTION OF FLUENCE IN THE DIFFERENT ZONES OF THE NPR-1 EXPERIMENT.

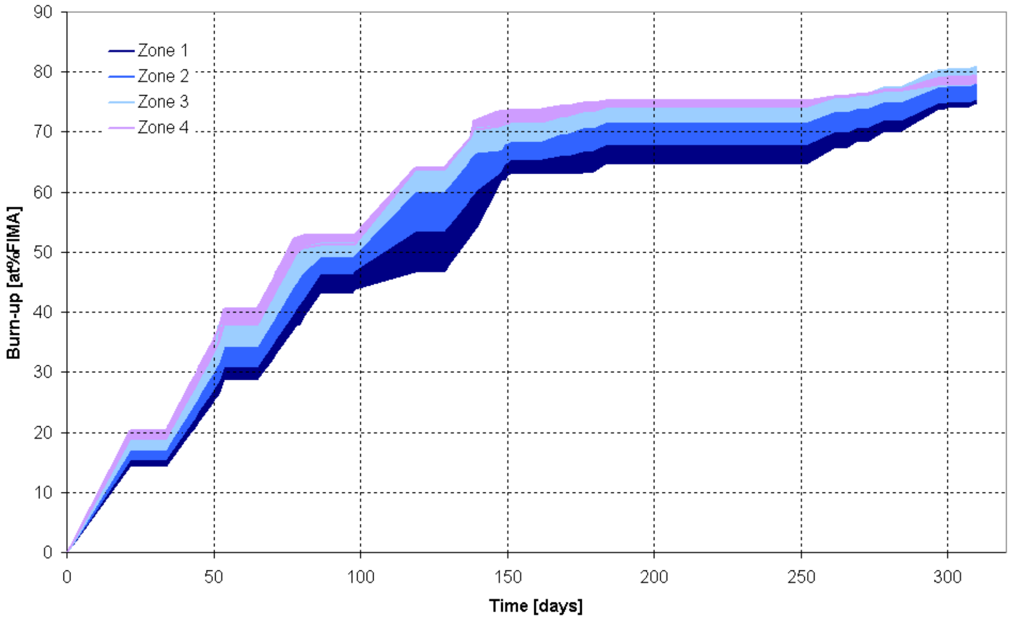

Figure 5: BURN-UP RANGE IN THE DIFFERENT ZONES OF THE NPR-1 EXPERIMENT.

2.3 EXPERIMENTAL RESULTS

2.3.1 Release-to-birth rate

The radiation detector consisted of two ionisation chambers. The system is sensitive enough to detect single particle failure. Samples of the sweep gas were also collected *periodically* and analyzed off-line. These measurements provided data used to calculate the release-to-birth rate of ^{133}Xe, ^{138}Xe, ^{85m}Kr and ^{88}Kr. No explanation is given on the way the release-to-birth rate were calculated. Data were provided by MAKI *et al.* [13]. Results are illustrated on Figure 6.

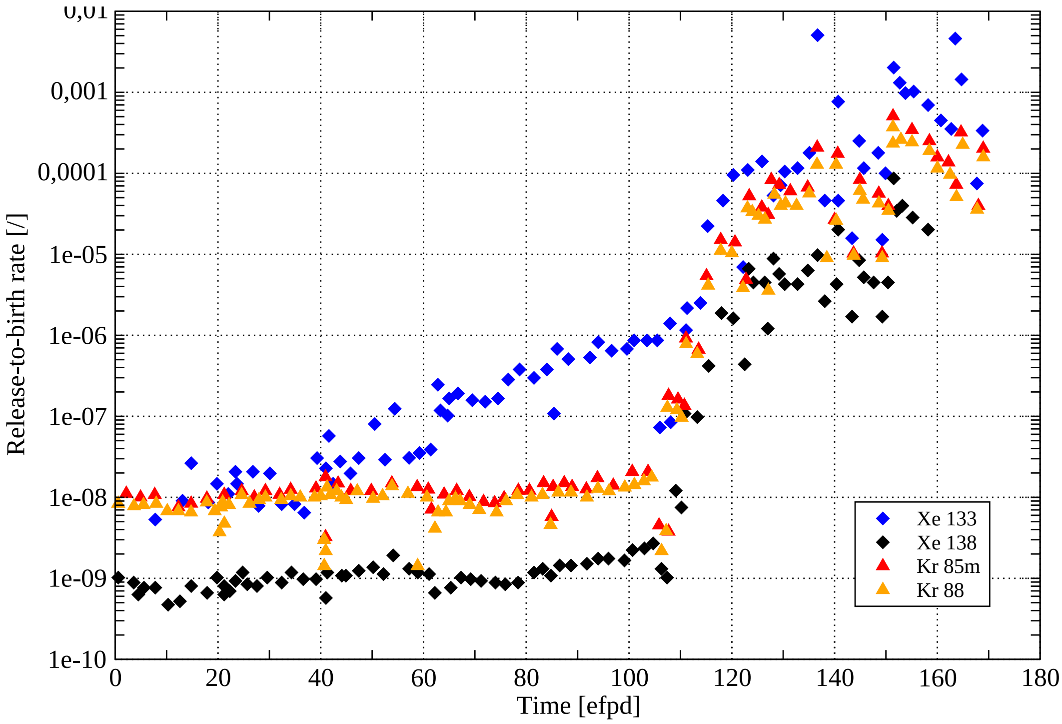

Figure 6: RELEASE-TO-BIRTH RATE OF VARIOUS GASEOUS FISSION PRODUCTS DURING THE NPR-1 EXPERIMENT.

This rate remained low, close to 10^{-8}, during the first 120 full power days. The first particle to fail, on January the 2nd 1992, created a R/B increase to 1.7 x 10^{-7} at a peak of fluence of 1.7 x 10^{25} n.m^{-2}. The ^{85m}Kr R/B continued to increase during the rest of the irradiation. It reached the final value of $\sim$ 3 x 10^{-4}.
At the end, **526 particles** were estimated to have failed (see below, 2.3.2).

2.3.2 Failure

The failures of the NPR-1 fuel were estimated by two methods:

- **Release-to-birth** measurements and its increase helped MAKI *et al.* [13], to estimate at **526** the number of failed particles.
- **Metallographic examinations** of two fuel compacts are reported by PETTI *et al.* [15]. According to these results, the number of failed particles (with broken SiC layers) ranges from near **0 to 3 %** of particles. These examinations also allowed to estimate the number of broken IPyC and OPyC layers. The metallographic examination results are summarized in Table 2 and represented on Figure 7. The high number of failure for the IPyC and OPyC layers should be denoted.

Compact	Layer	Sample Size	Failures (%)	95% Confidence interval (%)
A5	IPyC	39	31	$17 \leq P \leq 47$
	SiC	178	0.6	$P \leq 3$
	OPyC	39	90	$76 \leq P \leq 98$
A8	IPyC	53	6	$2 \leq P \leq 16$
	SiC	260	0	$P \leq 2$
	OPyC	53	47	$33 \leq P \leq 62$

Table 2: METALLOGRAPHIC EXAMINATION FAILURE RESULTS.

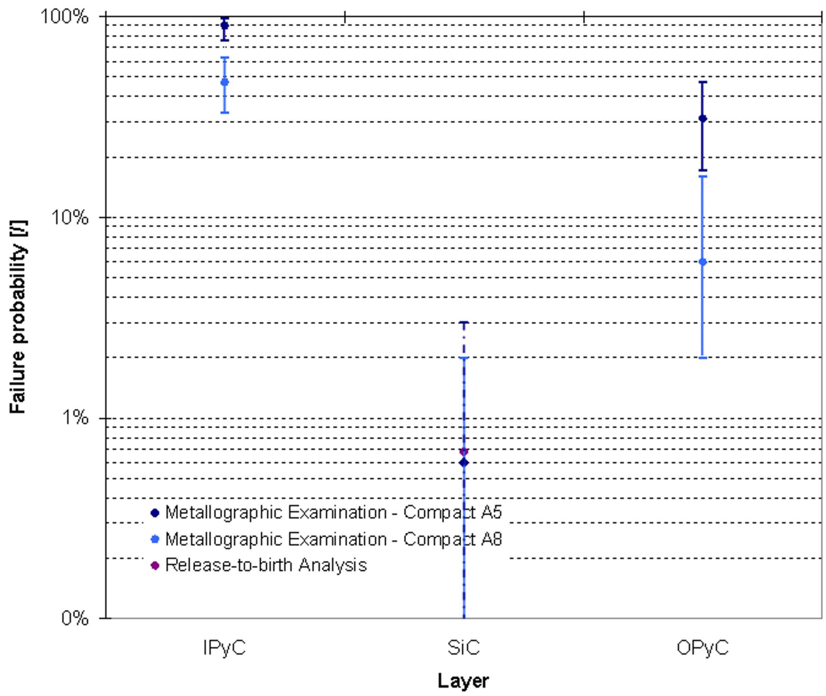

Figure 7: FAILURE EXPERIMENTAL RESULTS FOR THE NPR-1 EXPERIMENT.

2.4 ASSUMPTIONS AND DATA SET

2.4.1 Physical Assumptions

Kernel It has been assumed that no oxygen production happens, and so no carbon monoxide nor carbon dioxide are released from the kernel.

Fission products The enrichment of the NPR-1 fuel is very high, about 93%, and the fuel is used up to very high burn-up, over 80 at%FIMA. No available law are validated on this range of loads. As a result, the validity range of the following production per fission laws for Xe and Kr and their isotopes, have been extrapolated.

2.4.2 ATLAS data set

When properties or models are not available in ATLAS, assumptions have been made:

- as no properties nor models for UCO materials are available in the RAPHAEL2008 set of laws, the UO_2 materials properties are valid for UCO;
- as the enrichment of about 93% of the fuel exceeded the range available in the UO_2 model, no production per fission were taking into account. This term has been modified, according that the value has no great influence on the result. The following line has been added in the ADDITIONAL LINES part: `KRPERFISSION 0 '==' 1.E-6`

The set of data was generated thanks to an interface created between the HTR-Fuel Database and ATLAS. It will be as slightly modified as possible. The modification made are those recommended by Gauthier in [11]:

- no gap between the layers are modeled as their origins are unknown. It implies to reduce the Young's Modulus of the buffer to 1 MPa;
- to take into account the diffusion of the fission products out of the kernel during the irradiation. The following lines have been added in the ADDITIONAL LINES part:
  `--ACTIVITYDIFFUSIVITY 0 '==' 1.E-8;`
  where `--` is the fission product, `XE`, `XE133`, `XE138`, `KR`, `KR88`, `KR85M`, in this case.
- the external pressure during an experiment is set to 5 MPa with no variation in time as very few experimental data are available;
- The corrosion of the SiC layer by the Palladium (Pd) is not taken into account, because of the lack of data on it. The following lines have been added in the ADDITIONAL LINES part:
  ```
  * additional lines for the .ple files
  Var SiCPdCorrosion Int 0
  ```
- The amoeba effect won't be taken into account as no oxygen is released from the kernel. To disconnect this model, the following lines have been added in the ADDITIONAL LINES part:
  ```
  * additional lines for the .ple files
  Var KernelMigration Int 0
  ```

2.4.3 Probabilistic calculations

The probabilistic calculations have been done using the `bootstrap` method for statistical calculations. The following random variables were taken:

- **Layer thickness**, drawn in Truncated Gaussian functions,
- **Layer density**, drawn in Truncated Gaussian functions,
- **Fluence**, **irradiation Temperature** and **Burn-up**, drawn in *pseudo-uniform* functions.

The HTR-Fuel Data Base provides files only for 1D calculation and computation time is important for probabilistic calculation depending on the size of the sample. Samples of 200 x 200 x 200 particles or of 200 x 100 x 100 particles have been used, with one simulation per particle. Neither 2D nor 3D ATLAS simulations have been done.

2.4.4 Failure rate

The particle failure corresponds to the SiC layer one, meaning that studying the failure rate is equivalent to studying the SiC layer one. It can happen when the layer is subjected to tensile stress:

- early in the irradiation, because of the failure of one of the pyrocarbon layer changing its compressive effect on the SiC layer.
- at the end of the irradiation, due to irradiation-induced creep of the pyrocarbon. It reduces the compressive stresses in the SiC layer, which combined with increased internal pressure (due to gaseous fission products) leads to failure.

Two failure rates have to be examined: the SiC one alone and SiC one resulting of the PyC failure.

During a probabilistic calculation with ATLAS, the failure probability of each sample is calculated at the end of the whole set of simulations, assuming no failure occurs during the simulation. As a result, it is not possible to take into account the failure of one of the layers during the simulation. The failure probability is estimated in two steps as recommended in [10], Appendix B:

- probability that the PyC layer fails, assuming that the failure of the SiC does not happen: it is determined in the default case of a statistical simulation with ATLAS. It's expected to happen at the beginning of the life of the particle, when the failure of the SiC is negligible;
- probability that the SiC layer fails, assuming that the internal PyC layer is broken. The SiC failure is considered only if the PyC failure probability is not null at the time it happens. The properties of the failed layer are modified, in simulation, as follows:
  - ∗ the Young's modulus is reduced to the one of the buffer,
  - ∗ the diffusivity of the fission products is increased. It is made equal to the buffer one.

The probability of failure is calculated thanks to a Weibull law, whose coefficients are automatically generated by the HTR-Fuel-DB. The modulus, **m**, is 8.02 and the characteristic strength σ_{mean} is 873 MPa for the SiC layer. No parameters have yet been clearly chosen for the PyC.

2.5 CALCULATION RESULTS

The calculation results have to be compared with experiment data, two types of results have to be examined:

- the number of failed particles (PyC failed or SiC failed),
- the release-to-birth Rate, noted R/B Rate, for the different isotopes.

In ATLAS, the results are given as a function of FIMA when they are experimentally expressed as a function of full power day (efpd). It is necessary to transpose FIMA to efpd assuming they are related by a linear function.

2.5.1 Failure

The results are those of compact A5 and A8. The IPyC failure happens either at the very beginning of irradiation (with a probability of around 1.10^{-12}) or after 100 full power days of irradiation, as illustrated on Figure 8. The simulation is made in 3 steps: the first step of 200 samples, the 2 other steps of 100 samples .

With no PyC failed layer, the failure rate obtained is very low as presented in Table 3. The probability used is the **Identically Distributed sample estimator**, noted ID, described as the most accurate one [10].

Compact	Layer	Failures (%)	Variance (%)
A5	IPyC	7.94e-07	3.37e-12
	SiC	0.0	0.0
	OPyC	9.36e-08	2.93e-14
A8	IPyC	8.70e-07	1.39e-12
	SiC	0.0	0.0
	OPyC	1.25e-07	1.37e-13

Table 3: FAILURE RESULTS OBTAINED BY ATLAS.

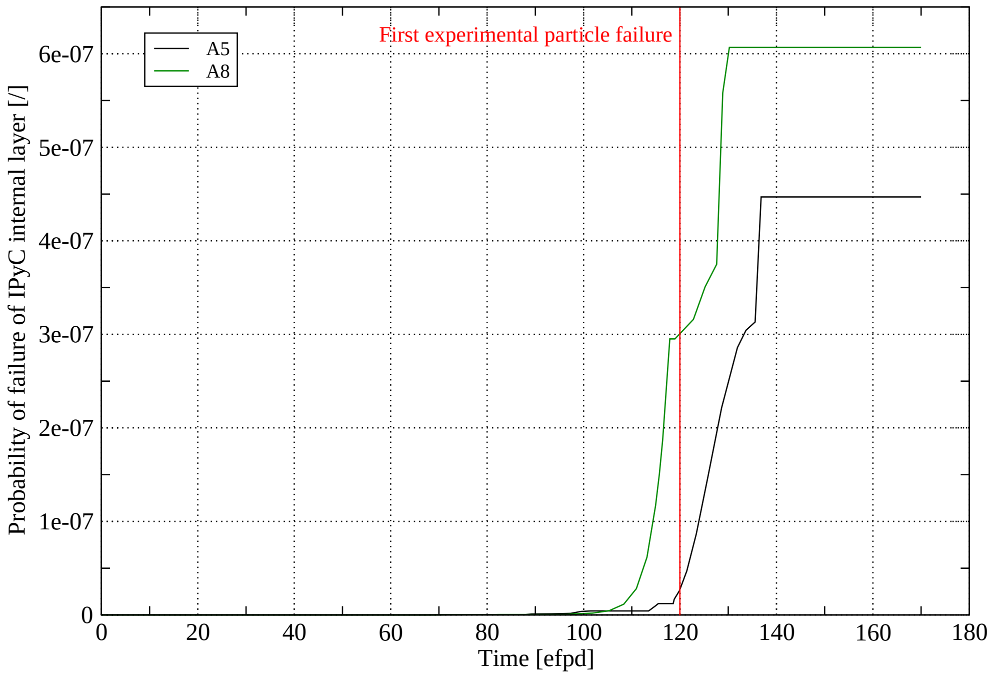

Figure 8: CALCULATED PROBABILITY OF FAILURE OF THE NPR-1 EXPERIMENT.

It has to be noted that, if the failure of the IPyC layer changes the stress state in the SiC layer but it has no influence on it in the Outer Pyrocarbon layer.

In order to evaluate the SiC layer failure rate, a second set of simulation is launched with IPyC layer properties modified, in order to consider it as failed, as described before. This simulation has 3 steps of 100 samples.

The probability for the OPyC layer does not significantly change.
The probability for the SiC layer stays null.

The probability calculated here is far too low but the coefficient used in the Weibull law do not correspond to this fuel. The generic parameters correspond to a German high quality SiC. In the NPR-1 experiment, the fuel is an American one, with less satisfactory performance [15]. The U.S. fuel is describe with a higher density, as more anisotropic than the German fuel which makes it more susceptible to crack under irradiation. It is supposed to explain the result's differences.

The documentation [9] shows that for Pyrocarbon, two laws are available, with different parameters (see Table 4):

- the **BNFL** law, whose parameters are given for ρ_0 = 1.73 $\mathrm{g.\ cm^{-3}}$, depending on the density. [1] gives others parameters for our density of 1.923 $\mathrm{g.\ cm^{-3}}$;
- the **CEGA** law, whose parameters depend on the BAF.

	Particular Parameter	m (/)	σ_{mean} (MPa)
BNFL	ρ_0 = 1.73 $\mathrm{g.\ cm^{-3}}$	7	190
	ρ_0 = 1.923 $\mathrm{g.\ cm^{-3}}$	5.2	220
CEGA	BAF = 1.058 (/)	9.5	446
Default	/	8.02	873

Table 4: PYC PARAMETERS FOR THE WEIBULL LAW.

The BNFL law for ρ_0 = 1.73 $\mathrm{g.\ cm^{-3}}$ will be called **BNFL 1** and the BNFL law for ρ_0 = 1.923 $\mathrm{g.\ cm^{-3}}$ **BNFL 2** in the rest of the document. A study with mean calculation gives the range of failure rate obtained for the different laws. The results are illustrated for the compact A5 on Figure 9 and they are summarized in Table 5. If the shape of the IPyC failure rate evolution remains the same, the value reached are very different. A factor of 10^7 exists between the two extremes.

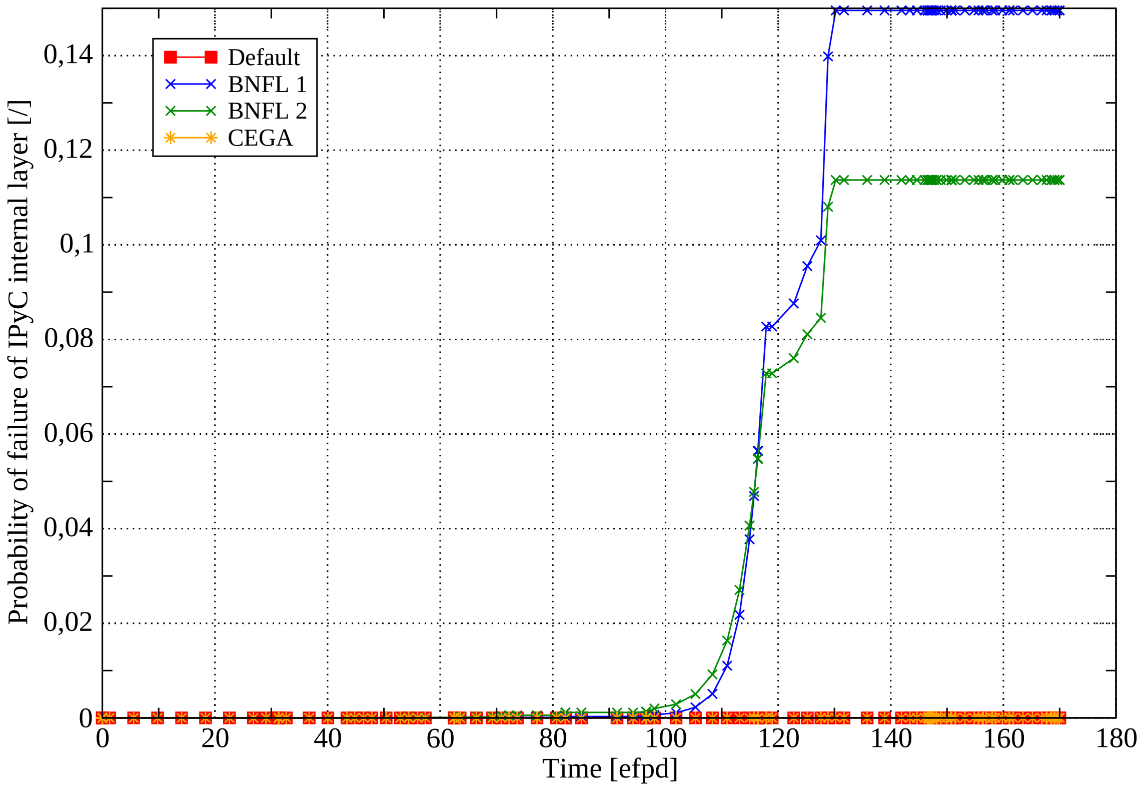

Figure 9: PROBABILITY OF FAILURE OF THE NPR-1 EXPERIMENT ON COMPACT A5 DEPENDING ON THE WEIBULL COEFFICIENTS.

Layer	Default	BNFL 1	BNFL 2	CEGA
IPyC	6.07 e-07	0.15	0.11	2.55e-05
OPyC	1.34e-11	1.40e-05	1.16e-04	7.82e-11

Table 5: MAXIMUM OF THE FAILURE RATE PROBABILITY, DEPENDING ON THE WEIBULL LAW COEFFICIENTS.

The results are the same for the two compacts. Whatever the chosen law, the failure rate of the SiC layer remains null.

The experimental high values are not those estimated. As the fuel (mechanical properties and behavior) is not well known, we can hardly go any further to improve our results. There is a difference of a factor **3** between the higher value estimated and the experimental results.

2.5.2 Release-to-birth Rate

The Krypton R/B rate is illustrated on Figure 10. The R/B rate is overestimated at the beginning of the irradiation and underestimated after the first experimental particle failure. The R/B rate of a particle with a failed IPyC layer is close to the rate of a particle with no failed layer.

The R/B rate of ^{85m}Kr and ^{88}Kr is estimated but it is lower than the experimental rate or than the rate calculated for Kr. The range of order are summarized in Table 6.

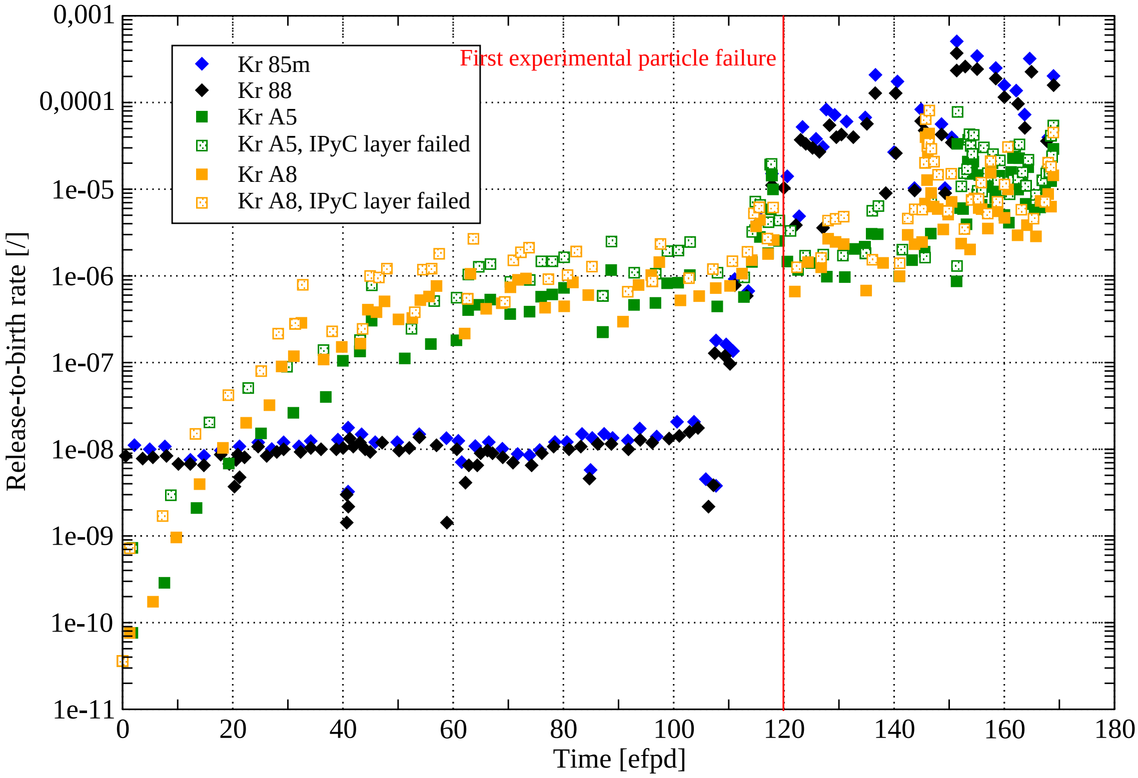

Figure 10: RELEASE-TO-BIRTH RATE FOR KRYPTON, EXPERIMENTAL DATA ARE DIAMONDS, ATLAS DATA ARE SQUARES.

	No failed layer			IPyC layer failed		
	Mean [/]	Min [/]	Max [/]	Mean [/]	Min [/]	Max [/]
Compact A5						
Kr	7.39E-6	2.94E-5	7.39E-13	1.29E-5	3.61E-4	8.22E-5
^{85m}Kr	9.33E-13	2.08E-11	2.99E-18	2.64E-11	2.94E-18	5.66E-10
^{88}Kr	5.02E-14	6.52E-13	5.49E-19	3.54E-12	2.79E-19	2.97E-11
Compact A8						
Kr	4.71E-6	7.38E-13	4.39E-5	8.32E-6	3.61E-11	8.07E-5
^{85m}Kr	3.39E-13	2.95E-18	3.52E-12	2.10E-11	3.92E-16	1.86E-10
^{88}Kr	1.67E-14	2.79E-19	1.77E-13	2.87E-12	1.79E-16	2.92E-11
Experimental Values	Mean [/]		Min [/]		Max [/]	
^{85m}Kr	4.12E-5		3.25E-9		5.07E-4	
^{88}Kr	2.63E-5		1.43E-9		3.71E-4	

Table 6: RELEASE-TO-BIRTH RATE OF KR, ^{85M}KR AND ^{88}KR OBTAINED BY ATLAS.

The Xenon R/B rate is illustrated on Figure 11. The estimation of the rate is good at the beginning of the experiment. As ATLAS does not consider the failure of a particle during a simulation, it is clear that the estimation is less accurate for the end of the irradiation.

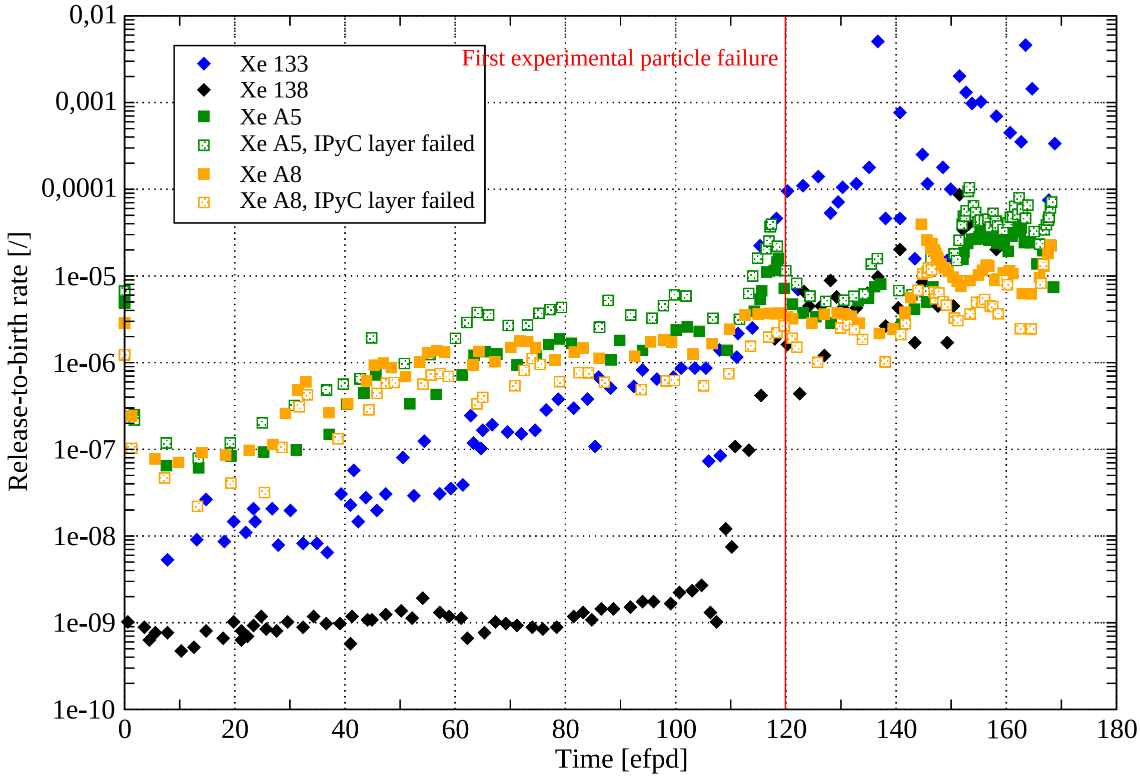

Figure 11: RELEASE-TO-BIRTH RATE FOR XENON, EXPERIMENTAL DATA ARE DIAMONDS, ATLAS DATA ARE SQUARES.

For the Xenon, our description is good at the beginning of the irradiation. After the first particle failure, at 120 efpd, our estimation is less accurate as no failure happens in the calculation but remains correct.

The R/B rate of ^{133}Xe and ^{138}Xe is estimated. It is illustrated on Figure 12 for the ^{133}Xe. The simulation gives a rate of one order of magnitude lower. Values of ^{138}Xe R/B rate are far lower than the experimental one. The different R/B rate for Xe and its isotopes are summarized in Table 7. Xe release-to-birth exceeds the overall R/B rate of the other isotopes: Xe is the initial filling gas.

For all the isotopes, the calculated probability of failure of the SiC layer is null and the release-to-birth rate for particle with a broken PyC layer is close to the rate obtained with a non-broken layer. Consequently, the estimation made does not correspond to the experimental results, after the first experimental particle failure which occurred after 120 full power days of irradiation.

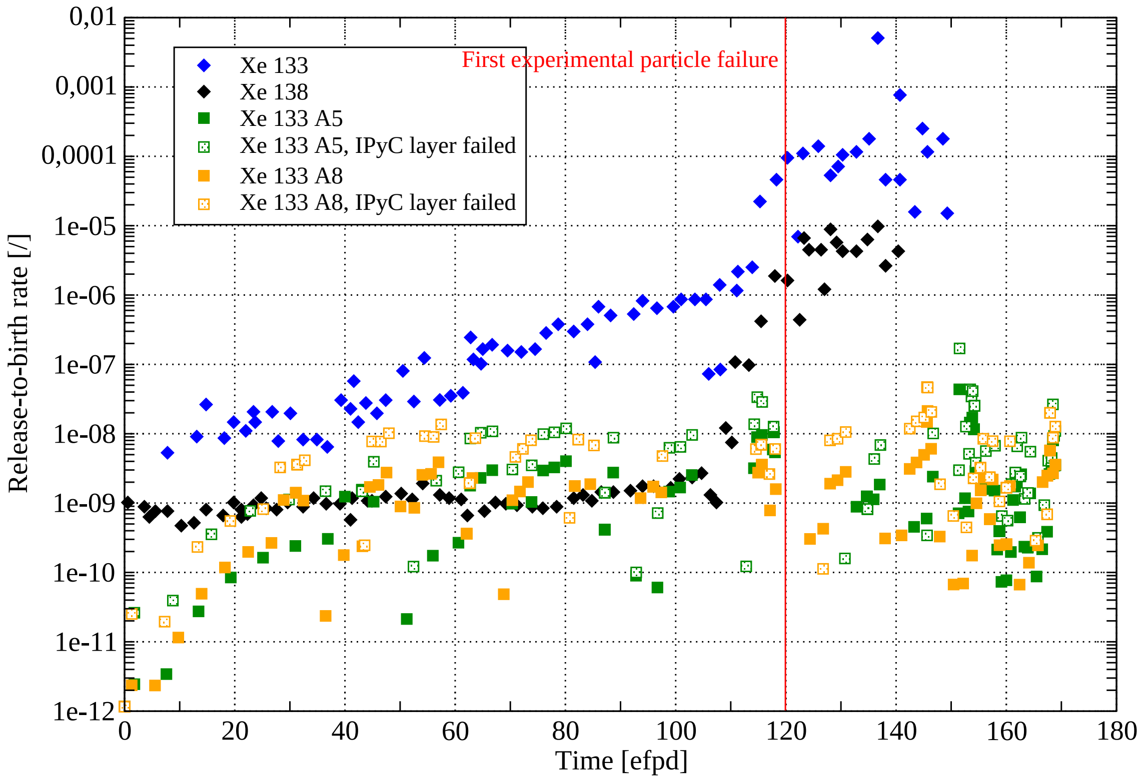

Figure 12: RELEASE-TO-BIRTH RATE FOR XENON 133, EXPERIMENTAL DATA ARE DIAMONDS, ATLAS DATA ARE SQUARES.

	No failed layer			IPyC layer failed		
	Mean [/]	Min [/]	Max [/]	Mean [/]	Min [/]	Max [/]
Compact A5						
Xe	7.39E-6	2.04E-8	2.77E-5	9.78E-6	6.73E-9	6.56E-5
^{133}Xe	2.53E-9	2.31E-14	4.36E-8	6.26E-9	1.16E-12	1.69E-7
^{138}Xe	2.69E-25	1.09E-43	8.76E-24	2.85E-20	6.03E-34	7.86E-19
Compact A8						
Xe	4.87E-6	6.79E-9	4.59E-5	8.66E-6	7.72E-8	8.14E-5
^{133}Xe	1.74E-9	2.31E-14	2.13E-8	5.55E-9	1.16E-12	4.71E-8
^{138}Xe	2.67E-25	3.04E-36	8.71E-24	2.94E-20	8.89E-29	7.84E-19
Experimental Values	Mean [/]		Min [/]		Max [/]	
^{133}Xe	2.04E-4		5.32E-9		5.07E-3	
^{138}Xe	4.39E-6		4.72E-10		8.65E-5	

Table 7: RELEASE-TO-BIRTH RATE OF XE, ^{133}XE AND ^{138}XE OBTAINED BY ATLAS.

2.5.3 Conclusion

Failure rate The failure probability has to be considered very carefully: the material parameters for American particles have to be better known and the Weibull law's parameters modified in consequence, before being able to estimate a realistic failure fraction. With default parameters, corresponding to German particles (and probably to newer particles) the estimation is too low and the result not reliable.

Release-to-birth rate As the release-to-birth rate calculated in a particle with a failed IPyC layer or without it stays close, it appears that in ATLAS, the fission products are mainly stopped by SiC layer.

With no particle failure, ATLAS provides a good estimation of the R/B rate of Xenon and of Krypton. The estimated R/B rate of the isotopes prediction is quite close to experimental result. The maximum difference between the results is close to a factor of 10^2, depending on the considered isotope.

3 HFR-EU1BIS

The HFR-EU1bis experiment was performed by JRC Institute of Energy in the HFR Petten reactor. Its objectives were to test the HTR TRISO particles from German pebbles at very high temperatures. This irradiation and some analysis are integrated in the HTR-F/F1 and other analysis are included in the RAPHAEL Projects. Most of the data used here to simulate the HFR-EU1bis experiment have been found in an HTR-F1 project deliverable from FÜTTERER, MARMIER and BERG [8]. Other data may be found in a technical report from FÜTTERER *et al.* [7] or in the Irradiation Progress Report from FÜTTERER [3, 4, 5].

3.1 DESCRIPTION OF THE EXPERIMENT

3.1.1 Sample Holder

The HFR-EU1bis sample holder was irradiated in the HFR core position G3 (see Figure 13). A schematic view of the sample holder is presented on the Figure 14; it's a standard device in the HFR Petten, called the "Full size HTR Fuel Element Rig" (ref. REFA-170). The sample holder constitutes the second containment. The first containment is an AISI 321 capsule; in this capsule the fuel pebbles are hold in place by graphite half shells (ref. SGLR6650). The pebbles are numbered from GLE4.1 to GLE4.5, from the top to the bottom of the capsule.

3.1.2 Loads Control

The experiment was designed to keep constant the temperature in the center of the pebbles, despite the decrease of power with time. The temperature of the pebble center was controlled by measuring the temperature of the surface of the pebble and adjusting the partial pressure of a helium-neon mixture of the coolant. The sample holder was turned by 180° cycle-by-cycle in order to reduce the radial gradients in neutron fluence and burn-up across the pebbles.

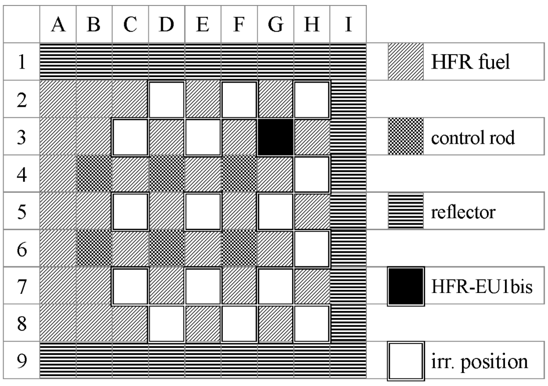

Figure 13: STANDARD REPRESENTATION OF THE HFR CORE.

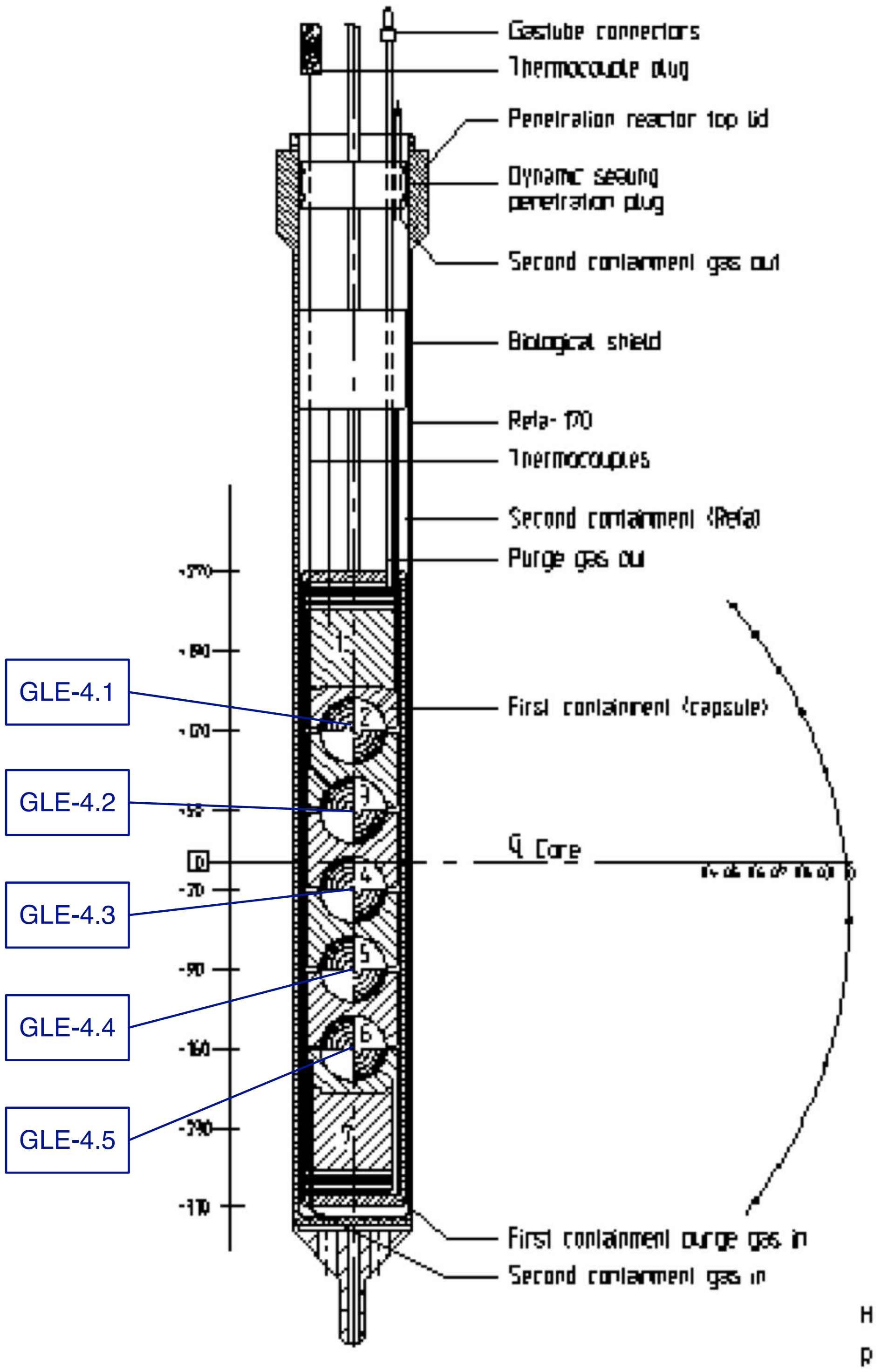

Figure 14: HFR-EU1BIS SAMPLE HOLDER.

3.1.3 Fuel

The HTR fuel element inserted in the HFR-EU1bis capsule was from former German production; LEU-TRISO particles with UO_2 kernels are inserted in pebbles. The fuel elements were from the AVR-GLE4/2 design; the particles were from the HT354-383 batch. The Graphite matrix was made of **A3-3 Graphite**. The characteristics of the HT 354-383 batch are summarized in Table 8. The 'mean' and 'standard deviation' were obtained from fabrication measures summarized by NABIELEK, VERFONDERN and WERNER [14]. The 'Min' and 'Max' values are from the specifications for the fuel of the 170 Wth MODUL reactor which were summarized by PETTI *et al.* [15] and are originally from GONTARD and NABIELEK [12].

Layer	Characteristic	Mean	Standard Deviation	Min	Max
Material	UO_2				
Kernel	Enrichment (^{235}U WT%)	16.75	N/A	N/A	N/A
	Radius (μm)	250.5	5.4	240	260
	Density ($g.\ cm^{-3}$)	10.85	N/A	10.4	*10.9**
Buffer	Thickness (μm)	92	14.3	72	108
	Density ($g.\ cm^{-3}$)	1.013	N/A	*0.95***	1.05
IPyC	Thickness (μm)	38	3.4	30	50
	Density ($g.\ cm^{-3}$)	$\approx$ 1.9	N/A	1.81	2.01
	BAF (/)	1.029	N/A	1	1.1
SiC	Thickness (μm)	33	1.9	31	39
	Density ($g.\ cm^{-3}$)	3.2	N/A	3.18	*3.22***
OPyC	Thickness (μm)	41	3.8	25	45
	Density ($g.\ cm^{-3}$)	1.8	N/A	1.81	2.01
	BAF (/)	1.020	N/A	1	1.1
Material	A3-3 Graphite				
Geometry	Pebble				
Fuel Elemeny	Radius (μm)	30	N/A	N/A	N/A
	Density ($g.\ cm^{-3}$)	1.75	N/A	1.73	1.77
	Number of particles	9560	N/A	N/A	N/A
	Last fabrication Temperature ($^\circ C$)	1900	N/A	N/A	N/A

Table 8: CHARACTERISTICS OF THE HT354-383 PARTICLES BATCH AND GLE4/2 PEBBLES.

* No specification is given, so a value close to the theoretical density has been chosen.
** No value is given, this is a "pure guess".

3.2 HISTORY

3.2.1 Time

Available data and calculations summarizing the experiment are reported in Table 9 and plotted on Figure 15. The experiment is divided in 10 cycles. It began on September the 7th 2004 at 5:10 pm and ended on October the 18th 2005 at 8:00 am. Each cycle is followed by a shutdown, which duration is also summarized on Table 9. The irradiation lasted 249 full power days.
The total length of the experiment, from the beginning date to the finishing date is 402.62 days and the modeled cycles (cumulated length of the irradiation, the shutdown and the power increase and decrease) is 403.52 days; the difference is so of 0.2 % higher.
It has been assumed that the power of the test reactor increases during 3 hours before reaching the nominal conditions of each cycles: *these durations are added to the irradiation duration calculated*.

3.2.2 Fluence

The data for fluence are available in form of accumulated fluence at the end of each cycle; it's from post-cycle calculations from FÜTTERER, MARMIER and BERG [8], they are summarized on Table 9. The following assumptions have been taken:

- the neutron flux is assumed to be constant during the cycle;
- the neutron flux is assumed to increase linearly during the power increase and decrease;
- the fluence is assumed to be the same for all the five pebbles, as no more precise data are available. The difference in position and exposure of the pebble is probably taken into account in the given 23.14% variation coefficient [8].

	Cycle	Duration (efpd)	Fluence (10^{25} n.m^{-2}) (E > 0.1 MeV)	Shutdown (days)
1	04-08	24.97	0.357	3.19
2	04-09	24.72	0.350	58.92
3	05-01	25.99	0.419	2.27
4	05-02	25.67	0.410	2.17
5	05-03	25.29	0.411	2.28
6	05-04	25.67	0.408	51.59
7	05-06	24.26	0.389	2.74
8	05-07	25.19	0.424	25.63
9	05-08	22.19	0.382	2.40
10	05-09	25.60	0.431	/

Table 9: ACCUMULATED FLUENCE AT THE END OF EACH CYCLE.

The total fluence, according to the data is Φ = 3.98 10^{25} n.m^{-2}(E > 0.1 MeV) and the total fluence of the modeled cycles (irradiation and power increase and decrease) is of Φ = 4.00 10^{25} n.m^{-2}(E > 0.1 MeV). The fluence for the modelled cycles is so 0.5% higher. Variations are represented on the following Figure 15.

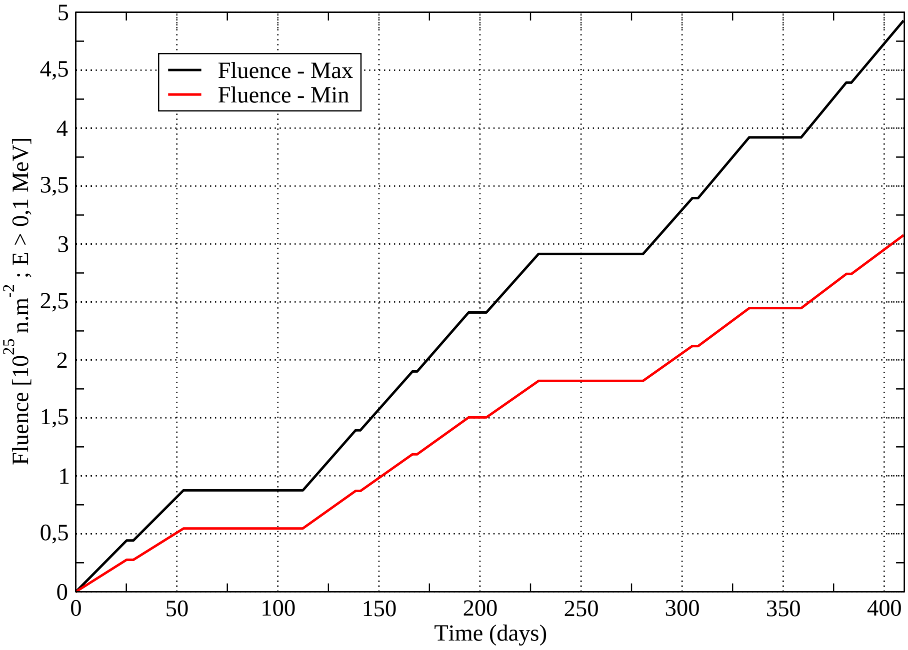

Figure 15: CYCLES AND FLUENCE FOR THE HFR-EU1BIS EXPERIMENT.

3.2.3 Burn-up

The available data for the burn-up are the following:

- a power for each pebble in each cycle from pre-irradiation calculations and corresponding estimated final burn-up. The calculated power is plotted on Figure 16;
- preliminary results for a measured burn-up, from BOTTOMLEY and FREIS [2].

The burn-up at **the end of the cycles** has been calculated in this document from the power using the following expression:

$$\tau_n^* = \frac{\dfrac{P_n\, d_n}{E}}{\dfrac{\mathcal{N}_A\, m_{HM}}{M_{U238} - e\,(M_{U238} - M_{U235})}} \tag{1}$$

With:

- n the number of the cycle,
- τ^* the burn-up at the end of the cycle (%FIMA), calculated from the power,
- P the power (W),
- d the duration of the cycle (s),
- E the fission energy for one particle (J). It has been taken E = 200 MeV(= 3.2 10^{-11} J),
- $\mathcal{N}_A$ the Avogadro number,
- m_{HM} the mass of heavy metal (g) with m_{HM} = 6 g,
- M the molar mass $(\mathrm{g.mol}^{-1})$,
- e the enrichment in ^{235}U.

By using this expression, it is possible to compare the burn-up calculated in [8], the burn-up calculated for this document and the burn-up measured in [2]. It is done in Table 10; the 'ratio' column contains the ratio of the measured burn-up over the burn-up calculated in this document.
Both calculated burn-up from the power are about the same (maximum difference: 1.6%): this validates the use of the expression 1. However, there is a high difference between measurements and pre-irradiation calculations: measured burn-up is about 75% of the calculated burn-up. As a result, the corrected burn-up history of the pebbles has been calculated from the calculated power assuming a proportional relationship (the corrected bun-up is plotted on Figure 17):

$$\tau_n = \tau_n^*(P)\,r \tag{2}$$

with r the ratio of experimental over calculated burn-up.

Pebble	Calculated [8]	Calculated here	Measured [2]	Ratio
GLE4.1	11.7%	11.9%	9.34%	0.79
GLE4.2	14.1%	14.2%	N/A	0.76*
GLE4.3	15.4%	15.4%	11.07%	0.72
GLE4.4	14.8%	14.7%	11.07%	0.76
GLE4.5	13.3%	13.5%	9.70%	0.72

Table 10: FINAL BURN-UP (AT%FIMA) IN THE PEBBLES, ACCORDING TO CALCULATIONS AND MEASUREMENTS.

* Because of the lack of measured burn-up, the ratio has been assumed to be the same as for the GLE4.4 pebble.

This allows to construct the burn-up history of each of the pebbles as a function of the time with the following assumptions:

- the probability of fission (derivative with time of the burn-up) is constant during the cycle. This is almost verified when looking to the reactor power histories given in [8];
- the probability of fission increases linearly with power during increases and decreases;
- the deviation is equal to the half of the difference in burn-up between neighboring pebbles, in order to calculate the minimum and maximum particle burn-up in each pebble.

History is plotted on Figure 18; maximum difference between experimental final burn-up and modeled final burn-up is 0.8%.

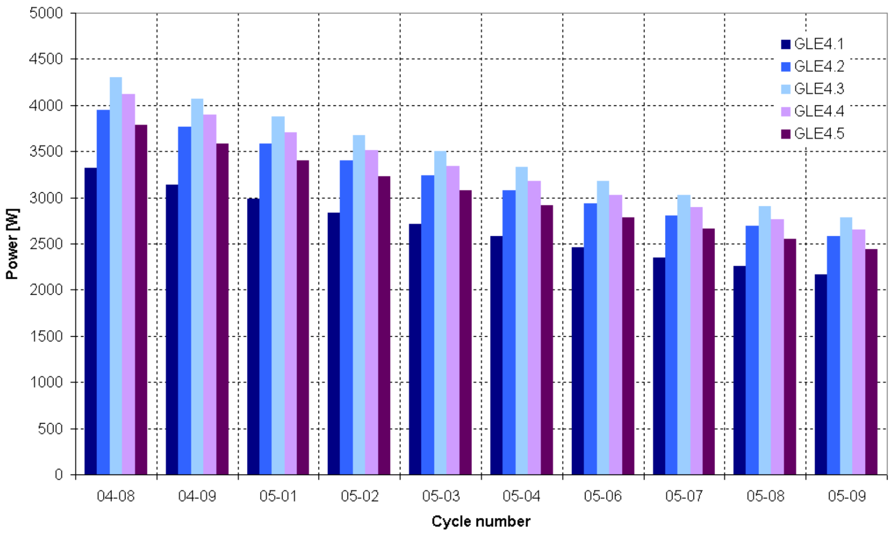

Figure 16: CALCULATED POWER IN THE PEBBLES, FROM PRE-IRRADIATION CALCULATIONS [8].

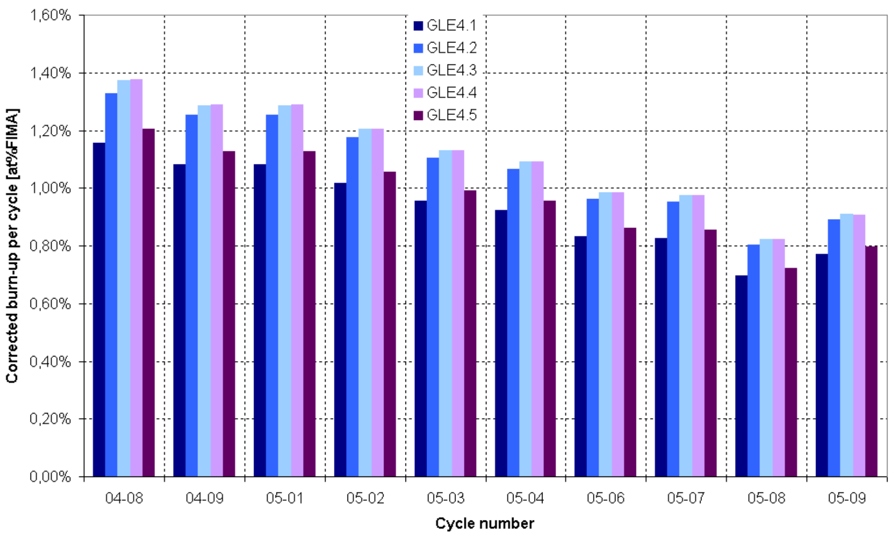

Figure 17: CORRECTED BURN-UP IN THE PEBBLES, FROM PRE-IRRADIATION CALCULATIONS AND PIE MEASUREMENTS.

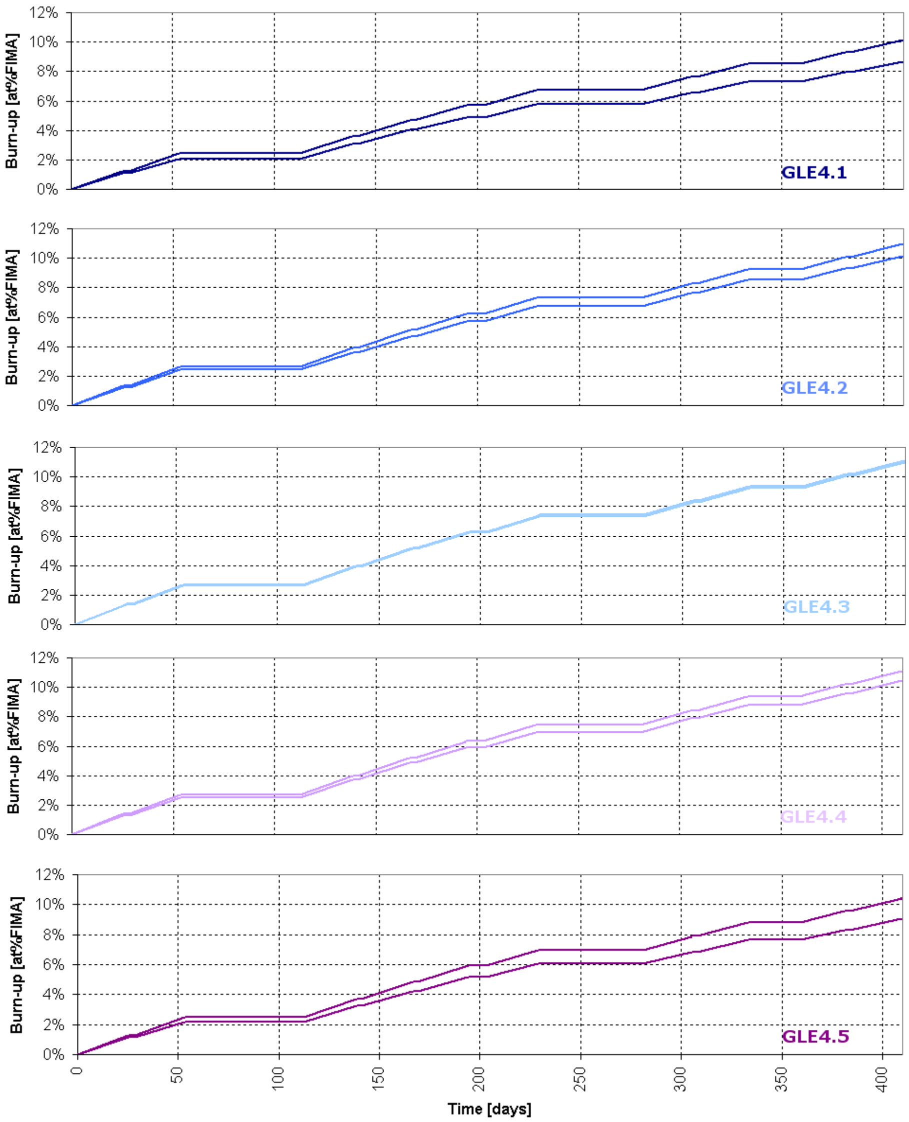

Figure 18: BURN-UP RANGES OF THE PEBBLES, FROM PRE-IRRADIATION CALCULATIONS AND MEASUREMENTS.

3.2.4 Temperature

Temperature measurements from 24 thermocouples are provided by FÜTTERER, MARMIER and BERG [8] during all the cycles; this thermocouples were placed in the graphite around the pebbles or on the pebble surface. The number of thermocouples per pebble ranged from 1 to 3. The temperature history has been simplified in order to be filled in the ODIN DATABASE and to make calculations with these results in an easier way. The following assumptions have been taken:

- the temperature is constant all over the cycle and is drawn between the maximum and minimum values. It's almost verified on the measurements of the temperature, even if in some cases, some regular increases or sudden steps are observed during the cycles;
- the minimum temperatures and maximum temperatures have been estimated by observing the differences between the different thermocouples for a compact (when it's the case) and the values reached all over a cycle (when increases of steps are observed);
- sudden temperature drops (of about 50°C to 200°C) observed haven't been taken into account for this preliminary qualification. They last for about one day and happen from 0 to 3 times per cycle.

The measured maximum temperature is the maximum temperature at the surface of the pebble. It is not representative of the temperature at the center of the pebble. To estimate the central temperature, the following calculations have been done:

$$T_C = T_S + \frac{P\,R^2}{6\,\lambda\,V} \tag{3}$$

With:

- T_C the central temperature ($^\circ$C),
- T_S the (maximum) surface temperature ($^\circ$C),
- P the (corrected) power in the pebble (W),
- R the radius (m) and V the volume (m^3) of the pebble,
- λ the Thermal Conductivity of the graphite Matrix ($\mathrm{W.\ m^{-1}{}^\circ C^{-1}}$)

The expression of the **Thermal Conductivity** of an **A3-3 Graphite** Matrix is taken from RAPHAEL2008 set of laws [13], its expression is:

$$\lambda(T,\Phi) = \lambda_0\,(1 - a_1(T - 273.15)\exp(-a_4(T - 273.15)))\,(1 - a_3(1 - \exp(-a_2\Phi) - a_5\Phi)) \tag{4}$$

Where:

- T the temperature (K),
- Φ the fluence (10^{25} n.m^{-2}; E > 0.1 MeV),
- $\lambda_0 = 50.8$, $a_1 = 1.181.10^{-3}$, $a_4 = 7.8453.10^{-4}$,
- $a_2 = 0.6(2.96 - 1.955.10^{-3}(T - 273.15))$, $a_3 = 0.94 - 0.604.10^{-4}(T - 273.15)$
- $a_3 = 0.6\left(4.3.10^{-5}(T - 273.15) - 8..10^{-3}\left(\frac{T - 273.15}{1000}\right)^8\right)$

The **Thermal Conductivity** used to calculate the central temperature is the mean of $\lambda(T = 800^\circ\mathrm{C}, \Phi)$ and $\lambda(T = 1200^\circ\mathrm{C}, \Phi)$ for the fluence Φ presented previously; as a consequence, *the Thermal Conductivity decreases with time*. The minimum and maximum surface temperatures and the calculated central temperature are reported on Table 11.

	Cycle	GLE4.1	GLE4.2	GLE4.3	GLE4.4	GLE4.5
1	04-08	S: 925-975 C: 1116	S: 950-1000 C:1162	S: 960-990 C: 1158	S: 970-990 C: 1158	S: 830-1030 C: 1177
2	04-09	S: 970-1050 C: 1193	S: 1000-1050 C: 1215	S: 975-1050 C: 1220	S: 990-1050 C: 1220	S: 900-1040 C: 1189
3	05-01	S: 900-1050 C: 1196	N/A	S: 850-1060 C: 1233	S: 875-1060 C: 1233	S: 880-1080 C: 1232
4	05-02	S: 880-1040 C: 1186	N/A	S: 900-1050 C: 1224	S: 950-1075 C: 1249	S: 850-1060 C: 1212
5	05-03	S: 980-1075 C: 1221	N/A	S: 975-1075 C: 1248	S: 1040-1080 C:1253	S: 980-1100 C: 1252
6	05-04	S: 980-1075 C: 1219	N/A	S: 1025-1080 C: 1251	S: 1040-1090 C:1261	S: 960-1120 SC: 1270
7	05-06	S: 990-1080 C: 1222	N/A	S: 1000-1100 C: 1268	S: 1050-1100 C:1268	S: 950-1160 C: 1307
8	05-07	S: 1020-1140 C: 1280	N/A	S: 1060-1170 C: 1235	S: 1070-1100 C: 1265	S: 1050-1200 C: 1345
9	05-08	S: 1020-1110 C: 1247	N/A	S: 1050-1120 C: 1282	S: 1080-1115 C: 1277	S: 1085-1165 C: 1307
10	05-09	S: 1035-1150 C: 1285	N/A	S: 1015-1210 C: 1369	S: 1085-1110 C: 1268	S: 1100-1180 C: 1319

Table 11: TEMPERATURE RANGE (°C) FOR EACH CYCLE (S: SURFACE TEMPERATURE; C: CALCULATED CENTRAL TEMPERATURE).

The single thermocouple of pebble GLE4.2 failed early in the irradiation. No data are available. It will be assumed that its temperature history is the same as pebble GLE4.4 because their temperatures were close before this failure.

3.3 EXPERIMENTAL RESULTS

3.3.1 Release-to-birth rate

For the HFR-EU1bis experiment, a gas measurement panel was installed in a glove box, for use about once a week. The samples were collected in a 100 cm^3 detachable sampling vessel, and were placed on an external multi-channel gamma spectrometer, calibrated to measure the concentration of following isotopes: 85^{m}Kr, 87Kr, 88Kr, 133Xe, 135Xe. Calculations of the disintegration of the isotopes during sampling allowed to obtain the concentration at the time of the sampling, and then neutronic calculations allowed to calculate the release-to-birth rate. The error is estimated to be successively about 4-9% for isotope concentration and 10-15% for the neutronic calculations. The Release-to-birth rate is given by FÜTTERER, MARMIER and BERG [8] in Figure 6 of the first part of the document, as a function of burn-up. An HFR-EU1bis Newsletter [6] provides the same Figure with a corrected burn-up according to experiments. According to the available data, and assuming constant fission rates during the cycles of the irradiation, the obtained release-to-birth rate has been calculated as a function of time and plotted on Figure 19.

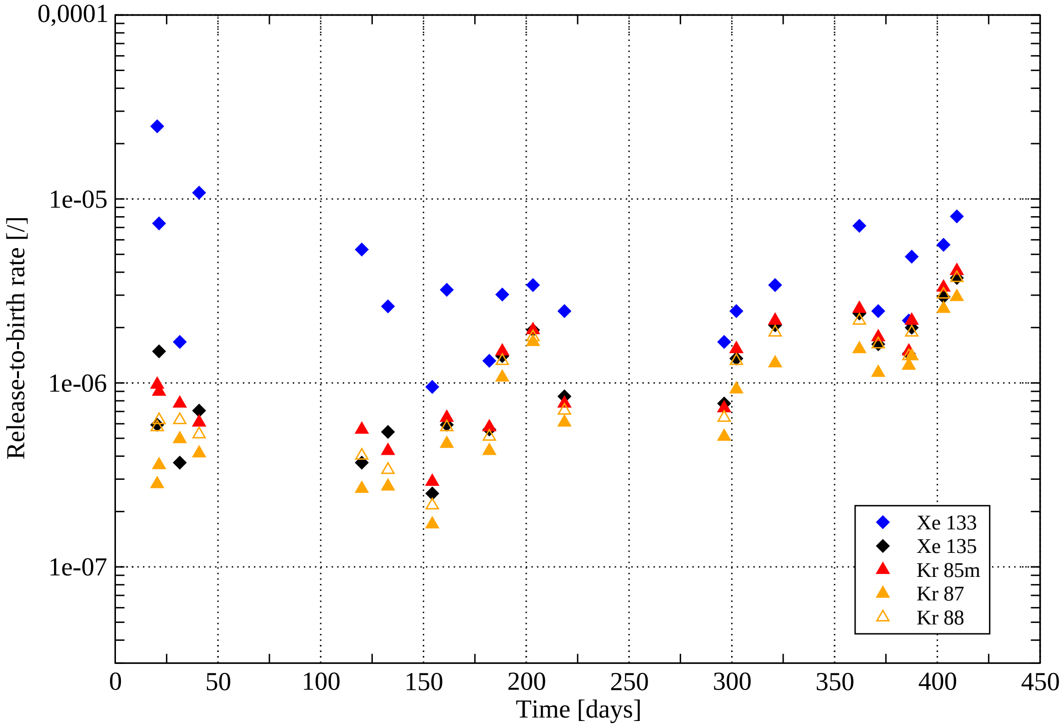

Figure 19: RELEASE-TO-BIRTH RATES AS A FUNCTION OF TIME, FOR VARIOUS FISSION PRODUCTS.

It should be noted that the higher release-to-birth for 133Xe is expected to be due to its additional precursors ^{133}I and ^{133m}Xe, as noted in [8].

3.3.2 Failure

According to the measurements, and the assumption made FÜTTERER, MARMIER and BERG [8] that the release-to-birth of a single failed particle is approximately 2x10^{-5}, no particle is expected to have failed during the experiment. But it shows that if no complete particle is expected to fail, some Pyrocarbon layer are expected to have failed.

3.4 MODEL ASSUMPTIONS

3.4.1 Recommendations

Assumptions and modifications made are mainly the same as those made in 2.4. However, the fuel is UO_2 and the porosity model needed some modifications.
The default law for porosity is:

$$P_0 = 1 - \frac{\rho_0}{\rho_{th}} \tag{5}$$

with, P_0 the initial porosity, ρ_0 the initial density and ρ_{th} the theoretical density, equal to 10.93 $\mathrm{g.cm}^{-3}$. In our case, the Kernel density, KERN_DENS is a variable parameter drawn in pseudo-uniform function, truncated between 10.4 and 10.9, with a mean at 10.85 and a deviation of 0.62.
Depending on the sample, the density can be close to the theoretical one after the shrinkage, leading to a small value for the porosity and so to the non convergence of the simulation. To consider the effect of the variation of the density after the shrinkage, the law has been modified. The following line has been added as particular conditions:

```
SHRINKAGE 0 '==' HEAVISIDE
SHRINKAGE 0 '*=' $-0.0023*min([1.,(1-KERN_DENS/10.93)/0.04])$
```

Calculations with the mean particle (mean densities, mean thicknesses,...) show no relevant difference between the default model and our model.

The probabilistic calculations have been done under the same assumptions and type of variables than in 2.4. The samples used were the same as those used in the simulation of the NPR1 experiment: (200, 100, 100) to estimate the PyC failure rate, (100, 100, 100) to estimate the SiC failure rate with failed IPyC layer.

3.5 Calculation Results

Mainly two types of results are to be examined:

- the number of failed particles, expected to be null,
- the Release-to-birth Rate for the different isotopes.

3.5.1 Failure

Same calculations as in section 2.5, in 2 steps have been made. No particle appears to fail. The IPyC failure probability keeps low (see Figure 20) but not null, as the OPyC layer (on Figure 21). This results have been calculated with the default Weibull law which correspond to a SiC material.

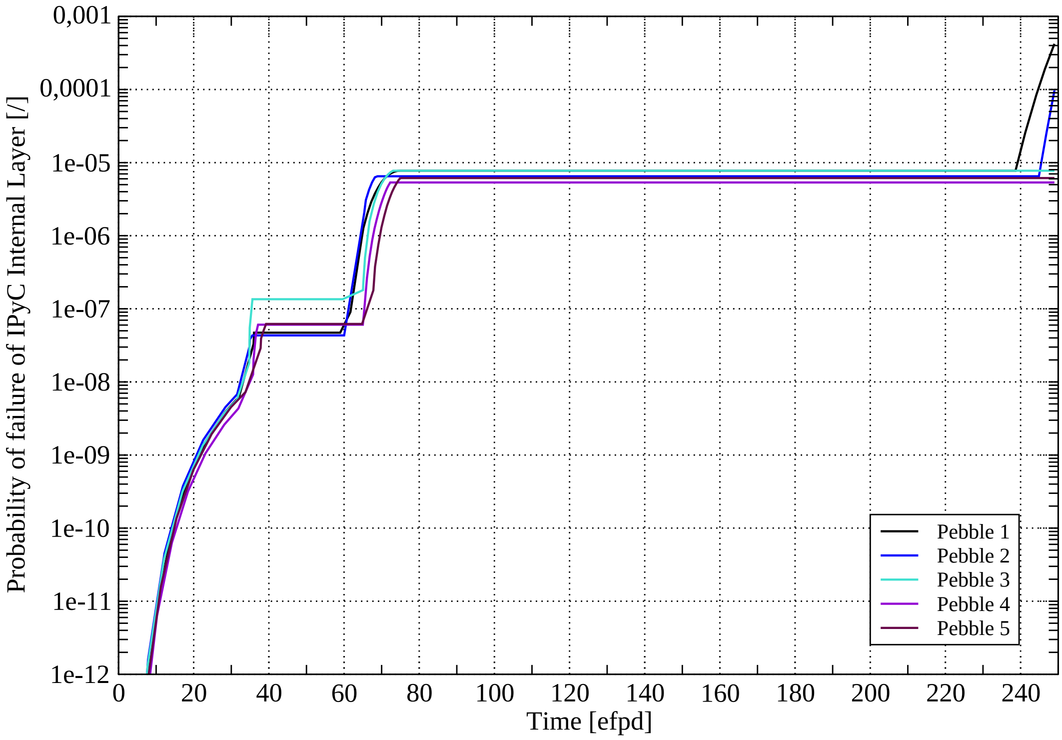

Figure 20: Probability of failure of the IPyC layer of the HFR-EU1bis experiment.

In the IPyC layer, for the five pebbles, the probability is quite the same, with the same evolution in time, except at the end of the irradiation where it reached its maximum, 4.10^{-3}, in the first pebble. During irradiation, the maximum, after 70 full power days, is close to 1.10^{-5} for all the pebbles.

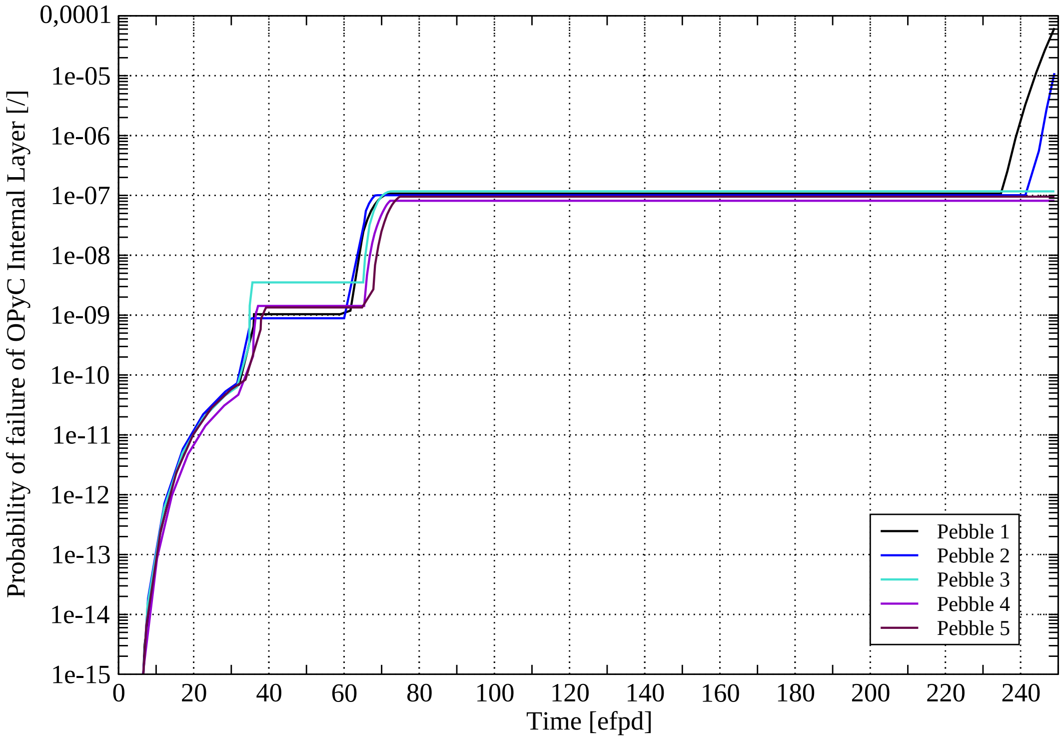

Figure 21: PROBABILITY OF FAILURE OF THE OPYC LAYER OF THE HFR-EU1BIS EXPERIMENT.

In the OPyC layer, the observations are the same, the probability is lower: its maximum is either close to 1.10^{-5} at the end of the irradiation or close 1.10^{-7} after 70 full power days.

Considering that there were 9560 particle per pebble and 5 pebbles, the probability becomes more significant.

Considering that the parameters used in the Weibull law are not those for Pyrocarbon, but that they should be (see 2.5.1):

- **m** = 5.2 and $\sigma_{\mathbf{mean}}$ = 220 MPa, for the **BNFL** law,
- **m** = 9.5 and $\sigma_{\mathbf{mean}}$ = 347 MPa, for the **CEGA** law.

The failure probability, as a function of the coefficients of the Weibull law, is illustrated on Figure 22, for the mean particle of pebble 1. The failure probability maximum was close to 1.10^{-5} (see Figure 20) if not taking into account the final peak, not representative of the other pebbles. Depending on the Weibull law, the maximum is illustrated on Figure 22 and is estimated for the mean particle to:

- $8.87 \cdot 10^{-5}$ with the default values,
- $4.97 \cdot 10^{-1}$ with the **BNFL** law,
- $6.62 \cdot 10^{-3}$ with the **CEGA** law.

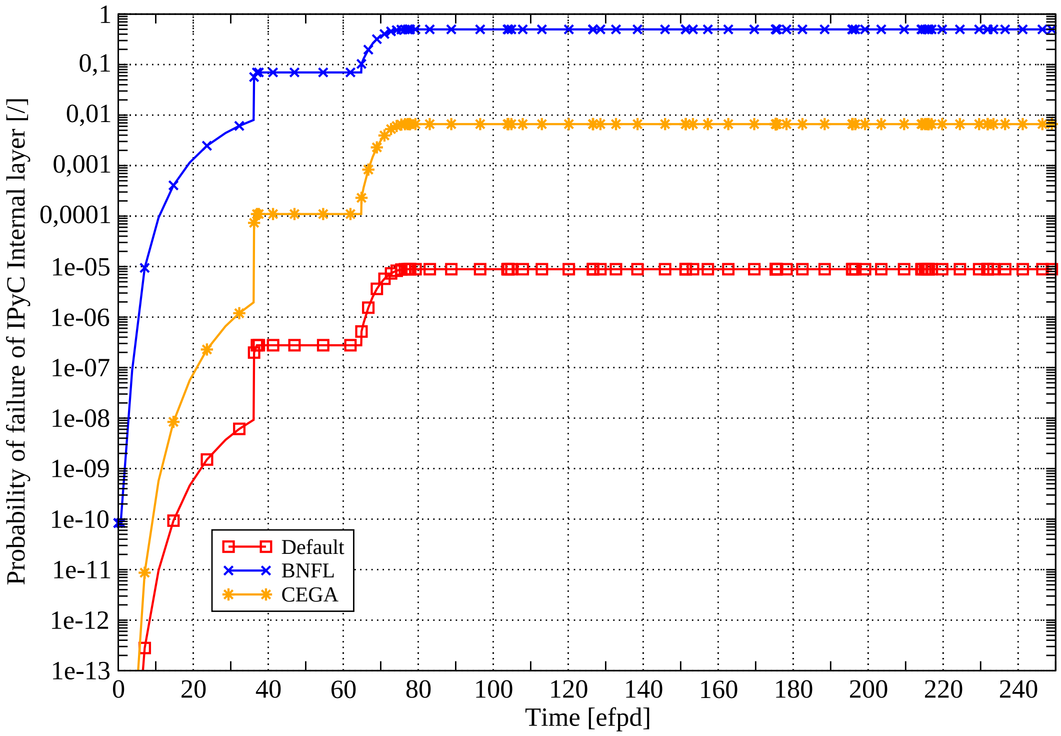

Figure 22: PROBABILITY OF FAILURE OF THE IPYC LAYER OF A MEAN PARTICLE OF THE HFR-EU1BIS EXPERIMENT WITH DIFFERENT CHARACTERISTICS IN THE WEIBULL LAW.

Simulation with an IPyC broken layer were conducted, as in section 2.5.1. It does not change the OPyC probability of failure and the SiC probability of failure remains null, as expected.

3.5.2 Release-to-birth Rate

Some diffusivity coefficients are too low, they are changed by the code ATLAS in order to improve the result. The R/B rate remains too low compared to measurements as illustrated on Figure 23 for Xe rate and Figure 24 for Kr one.

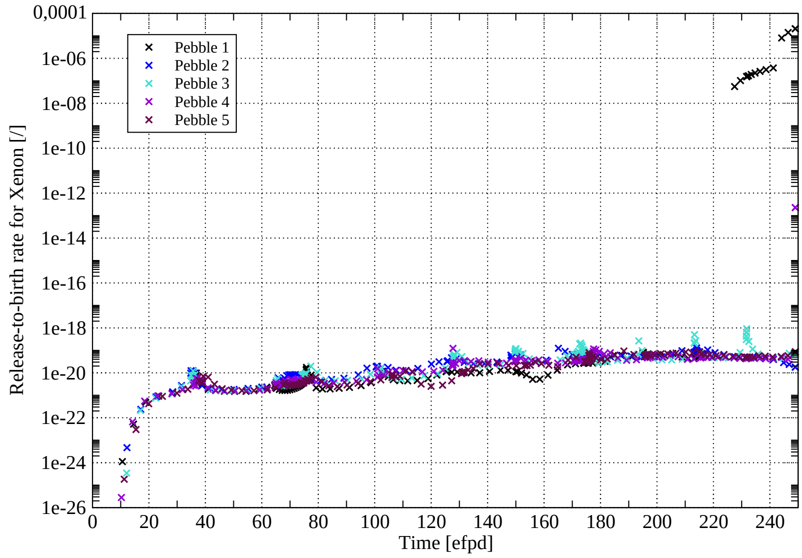

Figure 23: RELEASE-TO-BIRTH RATES AS A FUNCTION OF TIME IN THE DIFFERENT PEBBLES FOR XENON.

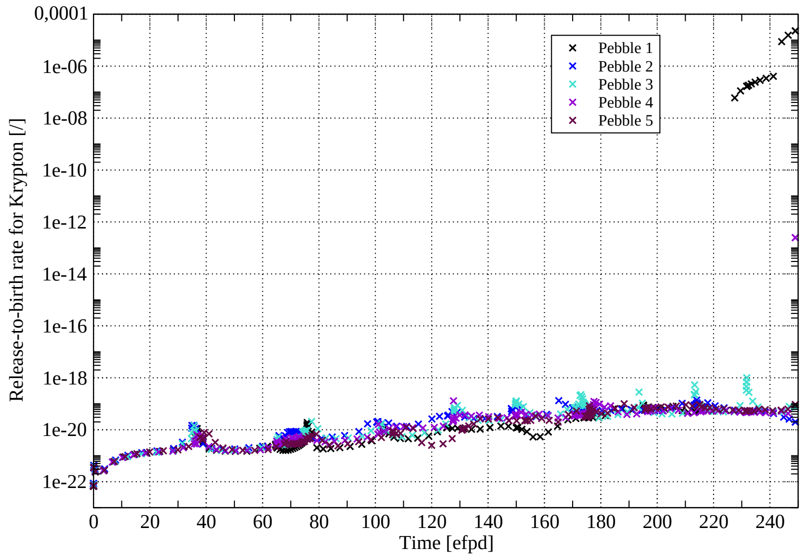

Figure 24: RELEASE-TO-BIRTH RATES AS A FUNCTION OF TIME IN THE DIFFERENT PEBBLES FOR KRYPTON.

The law for the coefficient diffusivity of the dense Pyrocarbon layers, for both Xe and Kr, used in ATLAS gives value smaller or equal to $1.3 \cdot 10^{-18}$ when equals to $1. \cdot 10^{-8}$ for the Porous Pyrocarbon and close to $1. \cdot 10^{-24}$ in the SiC layer. The temperature, the only variable of the law, may be too low compare to the validity range. By modifying those coefficients, the results can be improved.

It appears that there is a limit under which the R/B rate is very low and above which it reaches more expected values as illustrated on Figure 25. This limit is between $1 \cdot 10^{-11}$ and $1 \cdot 10^{-10}$.

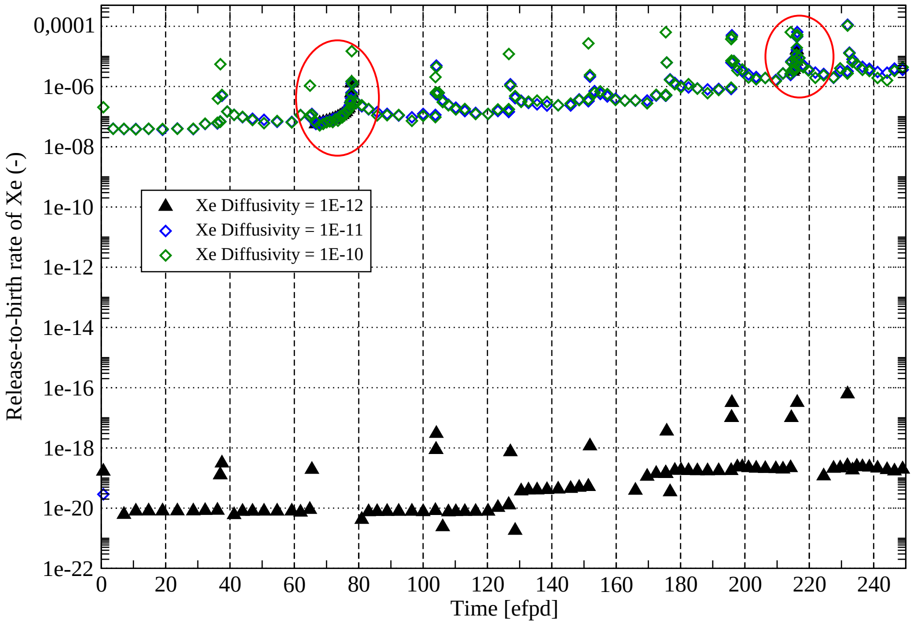

Figure 25: RELEASE-TO-BIRTH RATES DEPENDING ON THE DIFFUSIVITY COEFFICIENT OF PYROCARBON LAYERS.

With a diffusivity of $1 \cdot 10^{-11}$, a Release-to-birth rate of the order of magnitude of the experimental one is calculated (see Figure 26).

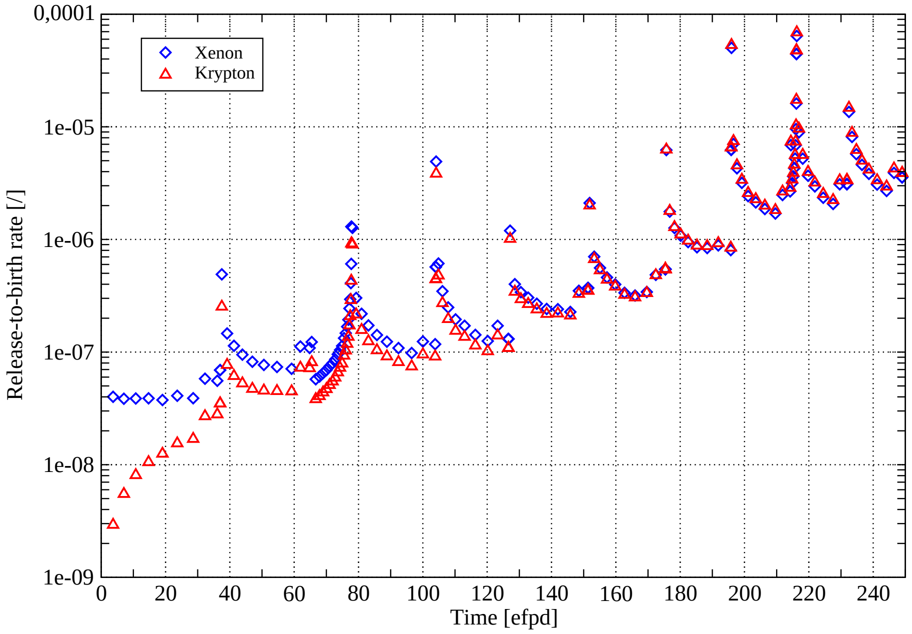

Figure 26: RELEASE-TO-BIRTH RATES WITH MODIFIED DIFFUSIVITY COEFFICIENTS.

3.5.3 Conclusion

Failure Some Pyrocarbon layers are expected to fail during irradiation. Whatever the chosen law, with no experimental data on the number of particle with failed layer, any of them gives a consistent result. In order to have the greatest estimation, to be in the worst case, the **BNFL** law has to be used.
However, the failure probability of the SiC layer remains null in a simulation with a deteriorate (broken) IPyC layer. The particle does not fail completely, as experimentally observed.

There is a good agreement between experimental and calculated results.

Release-to-birth rate As there are no precursors for Xe133 in ATLAS, its calculated R/B rate does not differ from the other isotope.
With a fitted diffusivity coefficient, the range of the R/B rate from experimental measurement and calculation covers the same range of values:

- between $1. \cdot 10^{-7}$ and $4. \cdot 10^{-6}$ for Kr,
- between $2. \cdot 10^{-7}$ and $3. \cdot 10^{-6}$ for Xe.

Both rates (experimental and calculated) have the same type of slow evolution. It should be noted that in the simulation the rates are estimated in full power days. In the experiment, the measurements are made in days. Thus, a comparison point by point cannot be made: the two time scales are different.

Nevertheless, with the fitted diffusivity coefficients ATLAS gives a good estimation of the release-to-birth rate for both isotopes.

4 CONCLUSION

A mean calculation, before a statistical simulation, should be made in order to verify the ATLAS messages. It helps to make sure that there is no models errors and also to:

- estimate the release-to-birth rate. If necessary, the concern law (production per fission for instance) or the diffusivity coefficients have to be modified;
- estimate the failure probability for different layer. With the interface, it is the SiC layer failure probability that is studied. If studying the PyC layer one, the coefficients of the Weibull law have to be changed by those of the **BNFL** law (depending on the density, see Table 12).

Density ($\mathrm{g.\ cm^{-3}}$)	m (/)	σ_{mean} (MPa)
1.73	7	190
1.95	5.2	220

Table 12: PYC PARAMETERS IN THE LAW FROM BNFL FOR THE WEIBULL LAW.

To evaluate the failure probability, the estimation has to be made in two steps:

- the first to evaluate the IPyC probability of failure (and to check if there are already some SiC failures with intact PyC), using the coefficients of the BNFL law (Table 12) in the Weibull law;
- the second, considering the IPyC as broken, to evaluate the resulting SiC failure probability, using the coefficients of the Weibull law given by default. They correspond probably well to SiC.

Using this method and these coefficients, the results obtained by ATLAS are consistent with experimental results.

Regarding the release-to-birth rate, some further studies are needed. For a non broken particle, the rate calculated gives a good order of magnitude.
Nevertheless, the response for all the isotopes is not good and the role and the influence of the diffusivity coefficients in the PyC layers have to be more precisely examined to understand the jump of the R/B rate.

List of figures

LIST OF TABLES

REFERENCES

[1] K. Bongartz, E. Gyarmati, H. Schuster, and K. Taüber. The brittle ring test : A method for measuring strength and young's modulus on coatings of htr fuel particles. *Journal of Nuclear Materials*, 62:123–137, 1976.

[2] D. Bottomley and D. Freis. Burn-up determination of HFR-EU1BIS, RAPHAEL WP3. Progress Meeting at ITU, Karlsruhe, 2008.

[3] M. A. Fütterer. HFR-EU1BIS: Irradiation progress report, cycles 04-08, 04-09, 05-01, 05-02. Technical Memorandum, HFR/05/4806, Project n° 337.2, rev.C, 2005.

[4] M. A. Fütterer. HFR-EU1BIS: Irradiation progress report, cycles 05-03, 05-04, 05-06, 05-07. Technical Memorandum, HFR/05/4812, Project n° 337.2, rev.B, 2005.

[5] M. A. Fütterer. HFR-EU1BIS: Irradiation progress report, cycles 05-08, 05-09. Technical Memorandum, HFR/05/4815, Project n° 337.2, rev.A, 2005.

[6] M. A. Fütterer, S. de Groot, and C. M. Sciolla. Preliminary results from an AVR fuel pebble irradiation at increased temperature and burn-up in the HFR Petten. In *Paper 5296, Proceedings of ICAPP '05, May 15-19, 2005, Seoul, KOREA*, 2005.

[7] M. A. Fütterer, H. Lohner, R. Conrad, K. Bakker, S. de Groot, and C. M. Sciolla. HFR-EU1BIS: Design and safety report. Joint Research Centre, D(04)11197, 2004.

[8] M. A. Fütterer, A. Marnier, and G. Berg. HFR-EU1BIS final irradiation report, HTR-F1 project, deliverable 2.1b. HTR-F1-06/09-D2.1.2, Draft, 2006.

[9] L. Gauthier. Analysis of models and properties of the dense layers of the htr fuel particle. Commissariat à l'Energie Atomique, NT SESC/LSC 09-013 - RAPHAEL DELIVERABLE D-FT4.6, 2007.

[10] L. Gauthier. Description of statistical approch and methods used in atlas v3.0. Commissariat à l'Energie Atomique, NT SESC/LSC 09-012, 2009.

[11] L. Gauthier. 'RAPHAEL2008', a reference set of models and properties for htr fuel particles calculations with atlas v3.0. Commissariat à l'Energie Atomique, NT SESC/LSC 09-018, 2009.

[12] R. Gontard and H. Nabielek. Performance evaluation of modern HTR TRISO fuels. HTA-IB-05/90, 1990.

[13] J. T. Maki, D. A. Petti, R. R. Hobbins, R. K. McCardell, E. L. Shaber, and F. H. Southworth. NP-MHTGR fuel development program results. Idaho National Engineering and Environmental Laboratory, INEEL/EXT-02-01268, 2002.

[14] H. Nabielek, K. Verfondern, and H. Werner. Selection of benchmark cases for mechanical failure prediction. HTR-F-04/08-D3.1.1, Draft, 2005.

[15] D. A. Petti, J. T. Maki, J. Buongiorno, R. R. Hobbins, and G. K. Miller. Key differences in the fabrication, irradiation and safety testing of u.s. and german triso-coated particle fuel and their implications on fuel performance. Idaho National Engineering and Environmental Laboratory, INEEL/EXT-02-00300, 2002.